Cretaceous Research 93 (2019) 292–317

Contents lists available at ScienceDirect

Cretaceous Research

journal homepage: www.elsevier.com/locate/CretRes

A revised chronostratigraphic framework for the Aptian of the Essaouira-Agadir Basin, a candidate type section for the NW African Atlantic Margin

Tim L. Luber [a, b, *], Luc G. Bulot [c, a], Jonathan Redfern [a], Mohamed Nahim [d], Jason Jeremiah [e], Mike Simmons [f, k], Stéphane Bodin [g], Camille Frau [h], Mike Bidgood [i], Moussa Masrour [j]

[a] University of Manchester, School of Earth and Environmental Sciences, North Africa Research Group, M13 9PL, Manchester, UK
[b] Equinor ASA, Martin Linges vei 33, 1364 Fornebu, Norway
[c] Aix Marseille Université, CNRS, IRD, Coll France, CEREGE, Aix-en-Provence, Site Saint-Charles - case 67 - 3, place Victor Hugo - 13331 Marseille cedex 3, France
[d] Office National des Hydrocarbures et des Mines (ONHYM), 34 Avenue Al Fadila, B.P. 8030 NU, Rabat, Morocco
[e] Golden Spike Geosolutions Ltd, SG2 9US, Stevenage, UK
[f] Halliburton, 97 Jubilee Avenue, Milton Park, Abingdon, OX14 4RW, UK
[g] Aarhus University, Department of Geoscience, 8000 Aarhus C, Denmark
[h] Groupement d'Intérêt Paléontologique, Science et Exposition, 60 bd Georges Richard, 83000 Toulon, France
[i] GSS (Geoscience) Ltd, 2 Meadows Drive, Oldmeldrum, Aberdeenshire, AB51 0GA, UK
[j] Université Ibn Zohr, Faculté des Sciences, Département de Géologie, Laboratoire de Géologie Appliquée et Géo-Environnement (LAGAGE), B.P 8106 Cité Dakhla, Agadir, Morocco
[k] The Natural History Museum, Cromwell Road, London, SW7 5BD, UK

ARTICLE INFO

Article history:
Received 12 September 2017
Received in revised form
19 August 2018
Accepted in revised form 12 September 2018
Available online 5 October 2018

Keywords:
Foraminifera
Calcareous nannofossils
Ammonoids
Carbon isotopes
Integrated stratigraphy
Sequence stratigraphy
Aptian
Essaouira-Agadir Basin
Morocco
Atlantic Margin

ABSTRACT

The Essaouira-Agadir Basin (EAB) of Morocco contains the most extensive exposure of Aptian to Lower Albian strata onshore the NW African Atlantic Margin. This paper documents the first high-resolution, multi-disciplinary stratigraphic approach for the Aptian to Lower Albian on the NW African Atlantic Margin. Previous biostratigraphic work almost exclusively relied on long-distance correlation of ammonoids to the Mediterranean – Caucasian Realm. Recent biostratigraphic work has questioned some of the previous interpretations, highlighting significant faunal endemism and complications with correlation to other key Aptian sections.

This study focuses on 5 key sections: Tiskatine, Id Amran, Assaka, and DSDP 416/370. Distribution of ammonoids, foraminifera, and calcareous nannofossils are reported from a bed-by-bed collection made at Tiskatine.

The analysis of foraminiferal and calcareous nannofossil assemblages enable correlation to standard zonation schemes; but also highlights the urgent need of revision and future work on the integration of these schemes across disciplines. The study, further, includes $\delta^{13}C_{carb}$, $\delta^{13}C_{org}$, and total organic carbon (TOC) data that is compared to reference material from the Vocontian Basin.

The combined litho-, bio-, chemo-, and sequence stratigraphic analysis establishes a robust chronostratigraphic framework for regional and super-regional correlations and a type section is proposed for the Aptian of NW Africa at Tiskatine.

1. Introduction

This multi-disciplinary stratigraphic study for the Aptian of NW Africa builds on the pioneering work of Kilian and Gentil (1906), Roch (1930) and Ambroggi (1963), which was focused on the bio- and litho-stratigraphy of the Essaouira-Agadir Basin (EAB). Additional work in the basin was carried out by Rey et al. (1986, 1988) and Witam (1998), but none of these studies proposed a high-resolution biostratigraphic framework. Yamina et al. (2002) provided a preliminary account on the distribution of Aptian planktonic foraminifera in the Western High Atlas in Morocco, although

* Corresponding author. University of Manchester, School of Earth and Environmental Sciences, North Africa Research Group, M13 9PL, Manchester, UK.
E-mail address: tllu@equinor.com (T.L. Luber).

https://doi.org/10.1016/j.cretres.2018.09.007
0195-6671/

this work lacked systematic descriptions or illustration. The work of Peybernes et al. (2013) has given some insight into ammonoid biostratigraphic distribution for the Aptian of the EAB, but the authors mainly compared their observations to the Standard Mediterranean Ammonite Scale (SMAS) of Reboulet et al. (2011, 2014), albeit highlighting the need for a local zonation scheme. This was addressed by Luber et al. (2017), who established a new ammonoid biostratigraphic framework for the EAB and selected Tiskatine as the type section for the Aptian in the west-central part of the basin, as initially suggested by Roch (1930). Two basin-wide hiatus were recognised spanning (*i*) the time equivalent of the middle part of the *D. forbesi* Zone to lower part of the *E. martini* Zone (SMAS), and (*ii*) the *H. jacobi* Zone and the lowermost part of the *L. tardefurcata* Zone (SMAS).

To support those findings, enable regional and super-regional correlations, and to build a robust bio-chronostratigraphic framework, this study presents an integrated stratigraphic approach for the Aptian of NW Africa. Excellent outcrop conditions at Tiskatine (Fig. 1) allow a bed-by-bed collection for combined ammonoid, calcareous nannofossil, and foraminiferal analysis, affording biostratigraphic calibration. This is integrated with chemostratigraphic data, including the first Aptian $\delta^{13}C_{carb}$ and $\delta^{13}C_{org}$ curves and total organic carbon (TOC) analysis for the onshore NW African Atlantic Margin. Two previously undocumented sections (Assaka and Id Amran) are described and are key in identifying local tectonic control on sequence development. The onshore sections are correlated to DSDP borehole 370, and a revised biostratigraphic analysis of the Upper Barremian to Lower Albian is presented.

This work also addresses correlation to the South Provence and Vocontian basins, key locations that establish the standard biostratigraphy of Mediterranean-Caucasian Subrealm *sensu* Westermann (2000) via the SMAS (Bergen, 2000; Kennedy et al., 2000; Moullade et al., 2000; Dauphin, 2002; Herrle and Mutterlose, 2003; Herrle et al., 2004; Kuhnt and Moullade, 2007; Baudin et al., 2008; Kennedy et al., 2014; Frau et al., 2015, 2017).

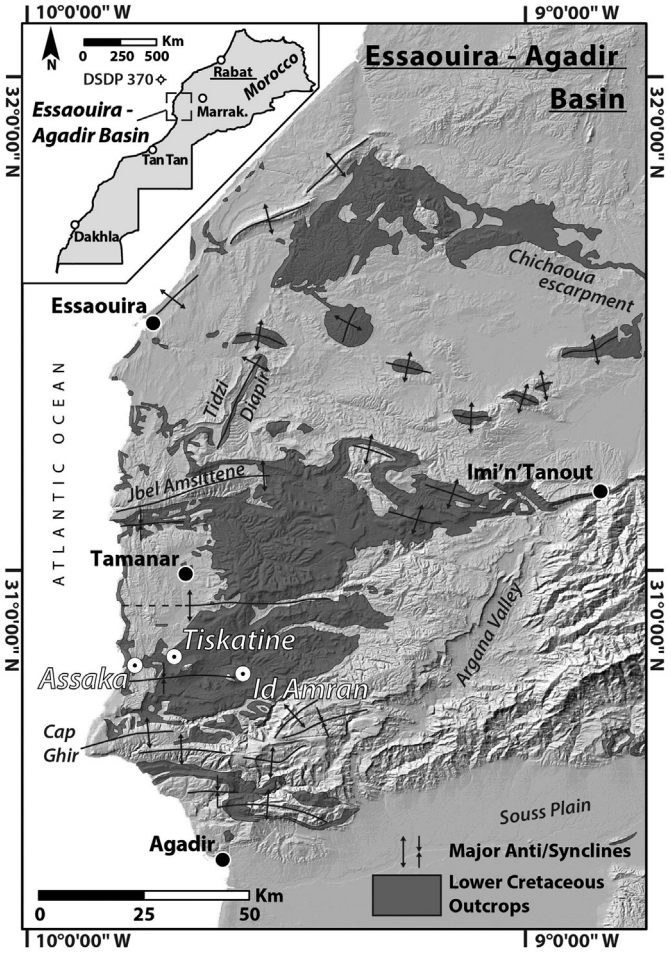

Fig. 1. Overview. **Inset:** Location map of Morocco and position of the DSDP well 370 offshore. **Main:** Digital elevation model of the Essaouira-Agadir Basin (EAB) with sections studied and sub-crop of the geological map showing Lower Cretaceous outcrops and main anticlines and synclines.

2. Regional setting and stratigraphy

During the Early Cretaceous the EAB was best described by a broad embayment, the "Atlas Gulf", above the Berriasian shelf opening out to the west into the proto-Atlantic (Behrens et al., 1978). Carbonate platform sedimentation that prevailed through most of the Jurassic continued into the earliest Cretaceous but was curtailed through flooding of the basin margin in the early Valanginian (Rey et al., 1988; Ettachfini et al., 1998). The EAB is limited to the north by the Meseta and the Jebilet, to the south by the Souss Basin, and to the east by the Massif Ancien de Marrakech. The modern-day exposure of the Mesozoic succession in the EAB occurs mainly along E-W trending anticlines and synclines linked to the Late Cretaceous to Cenozoic Atlasic orogeny (Laville et al., 2004) and combined salt tectonics (Tari and Jabour, 2013).

This work focuses on the Aptian of the west-central EAB. Studied sections are located within the Tiskatine syncline north of the prominent Cap Ghir anticline (Fig. 1, additional information in supplementary data). The lithostratigraphic framework is shown in Fig. 2 and has been discussed in detail in Luber et al. (2017). During the Late Barremian to Early Aptian (equivalent to the upper Bouzergoun Fm.), the region experienced a significant regressive phase (Nouidar and Chellai, 2001) (Fig. 2) leading to widespread exposure. Later during the Aptian (uppermost Bouzergoun Fm. to Tamzergout Fm.), transgression led to the developed of shallow-marine to open-marine shelfal conditions (Butt, 1982). Early Aptian (*P. dechauxi* Zone and potentially older) shoreface to shallow shelf conditions (upper Bouzergoun to lower Tamzergout Fm.) were followed by Late Aptian mid- to outer shelf conditions. The Aptian/Albian boundary is marked by an important regressive phase, followed by a return to shelfal conditions (Oued Tidzi Fm.) that persisted throughout the Early Albian (Butt, 1982; Rey et al., 1988).

2.1. Studied sections

2.1.1. Tiskatine (Sample-prefix: ***MTTK***)

Lat.: 30.821463° Long.: −9.702555° (Tiskatine 1) and Lat.: 30.810477° Long.: −9.739966° (Tiskatine 2).

A sedimentary log of the sections with field photographs of key intervals can be found in Fig. 3.

2.1.2. Id Amran (Sample-prefix: ***MTIA***)

Lat.: 30.796026° Long.: −9.571094°

A detailed log is presented in Fig. 4 and field photographs are shown in the supplementary data.

2.1.3. Assaka (Sample-prefix: ***MTAS***)

Lat.: 30.807297° Long.: −9.787837°

A detailed log of the section is shown in Fig. 5 and in the supplementary data.

2.1.4. DSDP Well 370 and 416

DSDP 370 – Lat.: 32.837500° Long: −10.776000° / **DSDP 416** – Lat.: 32.836300° Long: −10.801000°

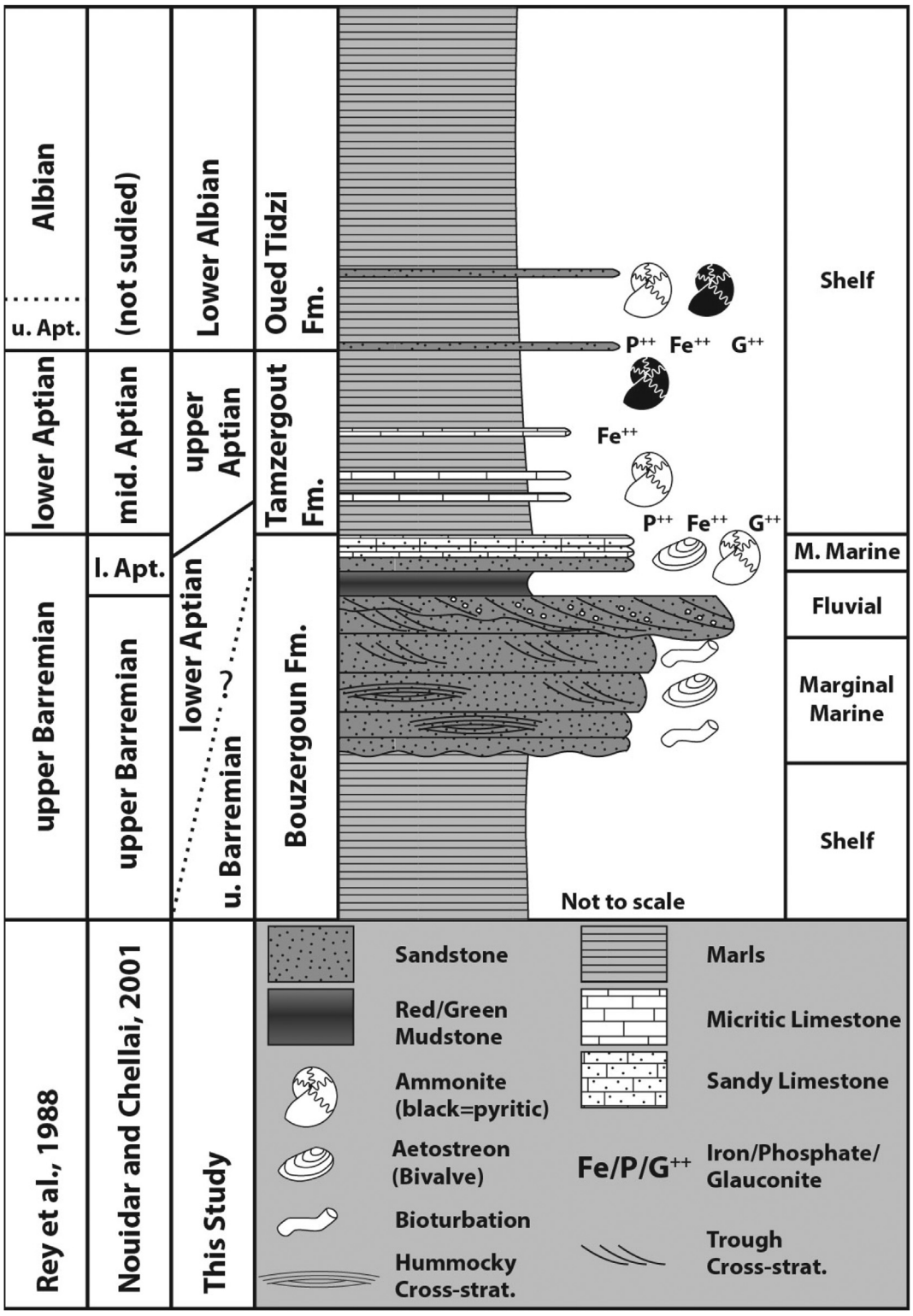

Fig. 2. Generalised lithostratigraphy of the Upper Barremian to Lower Albian strata in the west-central part of the EAB with broad depositional environments and key age interpretations.

To correlate the EAB outcrop stratigraphy offshore, the Upper Barremian to Lower Albian strata of DSDP boreholes 370 and 416 were sampled for calcareous nannofossils (request number: 049055-IODP and 049614-IODP). A summary log from borehole 370 is shown in Fig. 6. For sedimentary descriptions of this interval see Meyer (1978). DSDP 370 is located about 155 km offshore the modern Moroccan coastline in a water depth of 4214 m (Fig. 1). DSDP 416 is located 5 Km west of borehole 370.

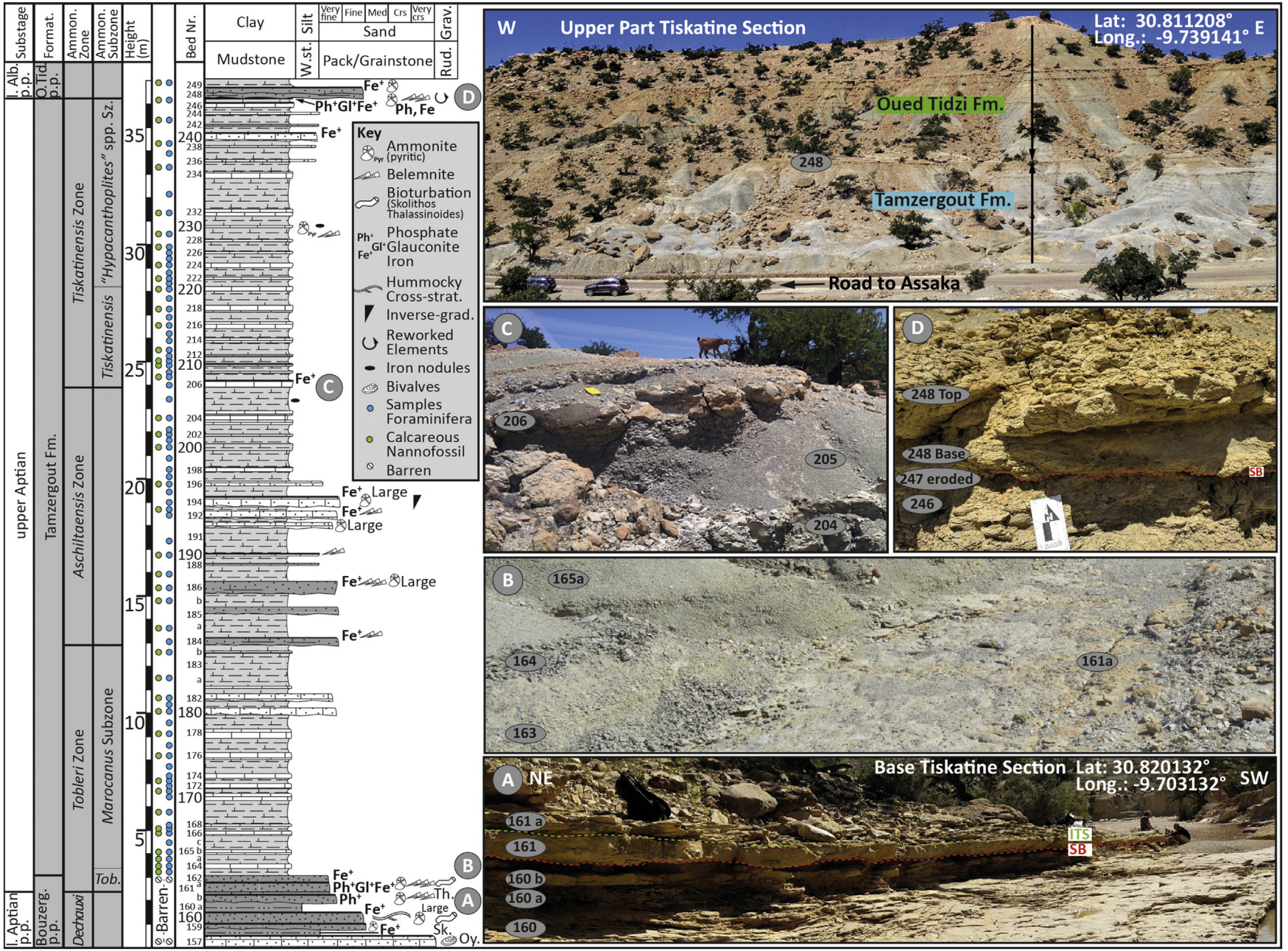

Fig. 3. Tiskatine section. Distribution of samples studied for foraminifera and calcareous nannofossil analysis and field photograph of key section intervals. Distribution charts can be found in the supplementary data. Abbreviations: Ammon. – Ammonite, Bouzerg. – Bouzergoun, grad. – grading, Grav. – Gravel, l. – lower, ITS – Initial Transgressive Surface, O. Tid. – Oued Tidzi, Oy. – Oyster, p.p. – pro parte, Rud. – Rudstone, SB – Sequence Boundary, Tob. – Tobleri, W.st. – Wackestone.

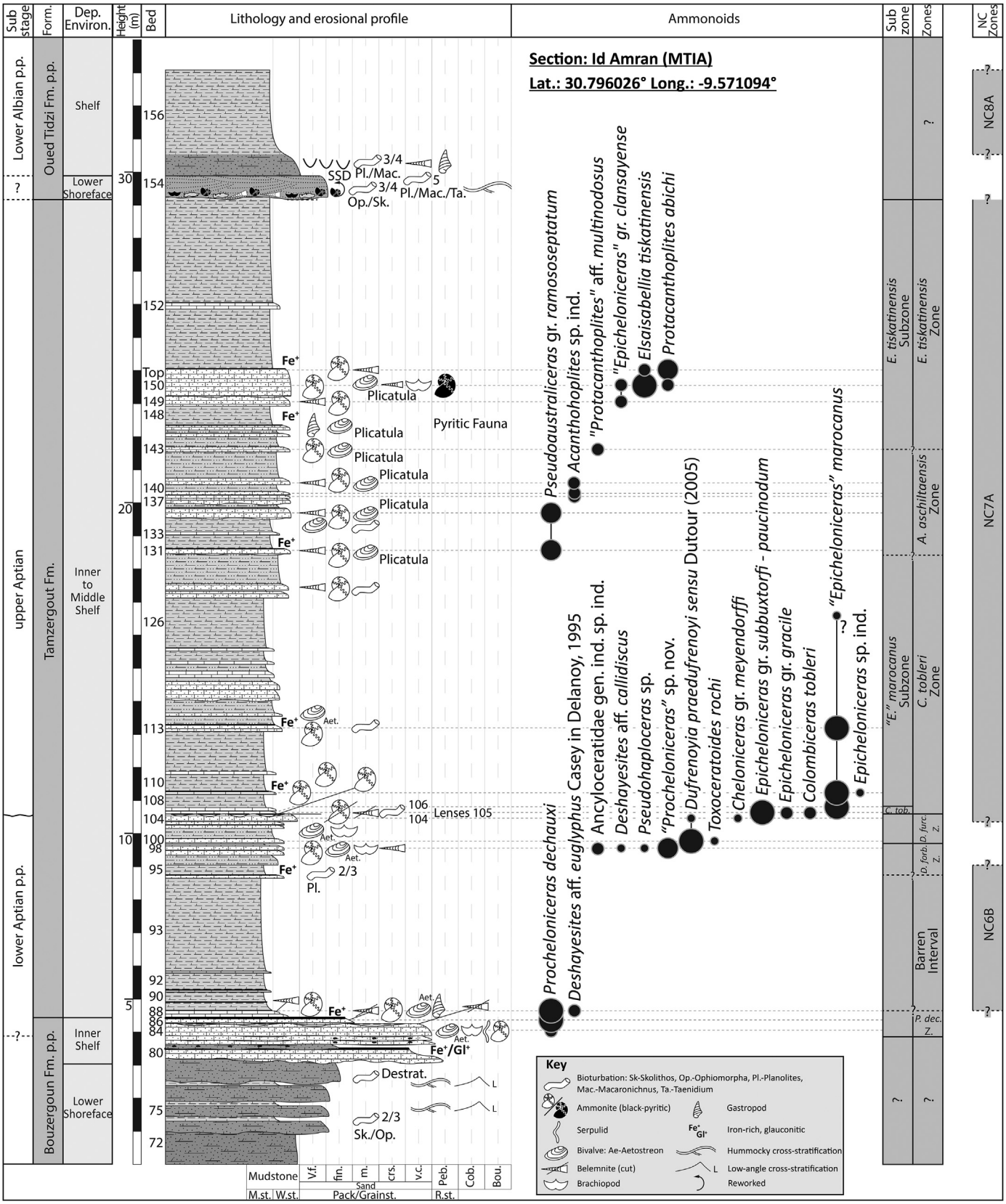

Fig. 4. Id Amran section. Distribution of ammonoids, key calcareous nannofossils, and biostratigraphic interpretation. Distribution charts for calcareous nannofossil can be found in the supplementary data.

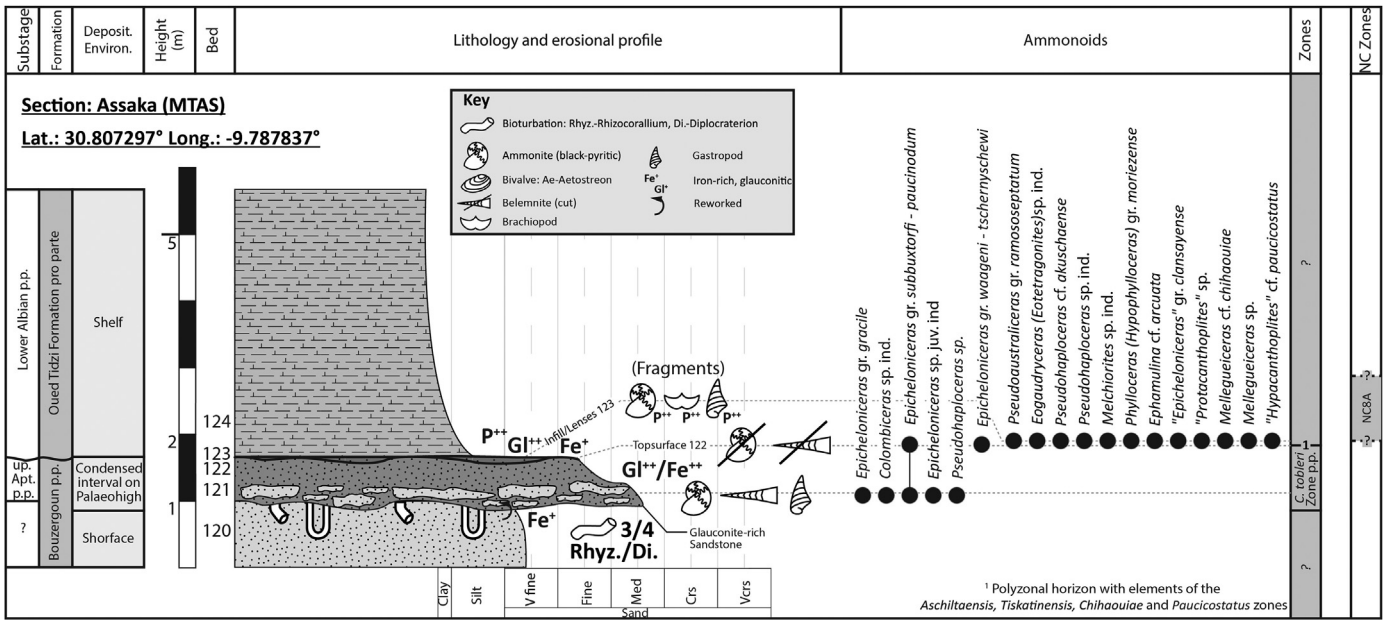

Fig. 5. Assaka section. Ammonoid distribution and biostratigraphic interpretation.

3. Methods

The lithostratigraphy, main depositional environments, and ammonoid biostratigraphy of the Tiskatine section have been described comprehensively by Luber et al. (2017). The Tiskatine section was sampled bed-by-bed for bio- and chemostratigraphic analysis. Most samples come from the Tamzergout Fm., with a few samples from the underlying Bouzergoun Fm. and the overlying Oued Tidzi Fm (Fig. 3). At the Id Amran and Assaka sections, key intervals were sampled for calcareous nannofossil analysis to support ammonite findings and extend observations made at Tiskatine. A list of all species recorded with primary citation information is presented in the supplementary data. New ammonoid findings, key foraminifera, and calcareous nannofossil species are fully illustrated for future reference.

3.1. Biostratigraphy

3.1.1. Foraminiferal biostratigraphy

Planktonic foraminifera have long been known to have stratigraphic utility within the later Early Cretaceous (e.g. Moullade, 1966) with a series of evolutionary inceptions and extinctions forming the basis for a standard planktonic foraminiferal zonation (e.g. Caron, 1985; Robaszynski and Caron, 1995; Premoli Silva and Verga, 2004; Ogg and Hinnov, 2012) shown in Fig. 7.

96 samples from the Tiskatine section were prepared using the standard methodology described by Armstrong and Brasier (2005). Microfossil recovery was good to very good (typically more than 100 and sometimes over 500 specimens) but variable. Preservation was generally good. Key specimens are illustrated in Figs. 8 and 9.

The taxa present comprise a diverse assemblage of calcareous and agglutinating benthonic foraminifera and planktonic foraminifera. Planktonic foraminifera often form 50% or more of the total assemblage. Notwithstanding considerable discussion of the taxonomy of Early Cretaceous planktonic foraminifera (BouDagher-Fadel et al., 1997; Moullade et al., 2002; Bellier and Moullade, 2002; Verga and Premoli Silva, 2003a; b; Premoli Silva and Verga, 2004; Ando et al., 2013) and remaining uncertainties regarding precise stratigraphic range, their fundamental stratigraphic utility remains. The taxa are identifiable with reference to the extensive literature on age-equivalent cosmopolitan, Mediterranean and North-West European material (e.g. Bartenstein and Bettenstaedt, 1962; Damotte and Magniez-Jannin, 1973; Premoli Silva and Verga, 2004). The identification of key planktonic foraminifera follows the taxonomy of Verga and Premoli Silva (2003a, b) and Premoli Silva and Verga (2004). Although the nomenclature of zonation varies between authors (e.g. use of *Hedbergella infracretacea* Zone or *Pseudoplanomalina cheniourensis* Zone instead of *Hedbergella trocoidea* Zone), the basic series of defining events is well understood. Direct calibration to other stratigraphic tools (e.g. the SMAS and carbon isotope record and hence the chronostratigraphic standard) is still at a very preliminary stage and remains a subject of ongoing research.

3.1.2. Calcareous nannofossil biostratigraphy

44 samples from the Tiskatine section were analysed via standard techniques described by Bown and Young (1998) and the picking brush method of Jeremiah (1996). At Id Amran a total of 8 samples where analysed for calibration to ammonite-bearing layers and as infill where ammonite recovery was poor or absent. Similarly, an infill sample was studied from Assaka. At DSDP boreholes 370 and 416, nineteen and 5 samples were investigated, respectively. Samples were analysed semi-quantitatively, with the first 30 fields of view counted and the remaining slide scanned for rare specimens. Key specimens are illustrated in Fig. 10.

The nannofossil biostratigraphy is described with reference to the Lower Cretaceous NC zones of Roth (1978, 1983) and subzones after Bralower et al. (1993). The standard Aptian nannofossil zonations are, however, in urgent need of revision. The nominate species utilised in the cosmopolitan NC zonation (Roth, 1978; Bralower et al., 1993) either show diachronism (FAD *Prediscosphaera columnata* (Stover, 1966), Fig. 10), difficulty of identification (differentiation of *Hayesites albiensis* Manivit, 1971 from *Hayesites irregularis* [Thierstein in Roth and Thierstein, 1972)] or a sporadic Last Appearance Datum (LAD) [*Micrantholithus hoschulzii* (Reinhardt, 1966)]. Therefore, the calibration of nannofossil zones as shown in standard texts (e.g. Ogg and Hinnov, 2012) requires

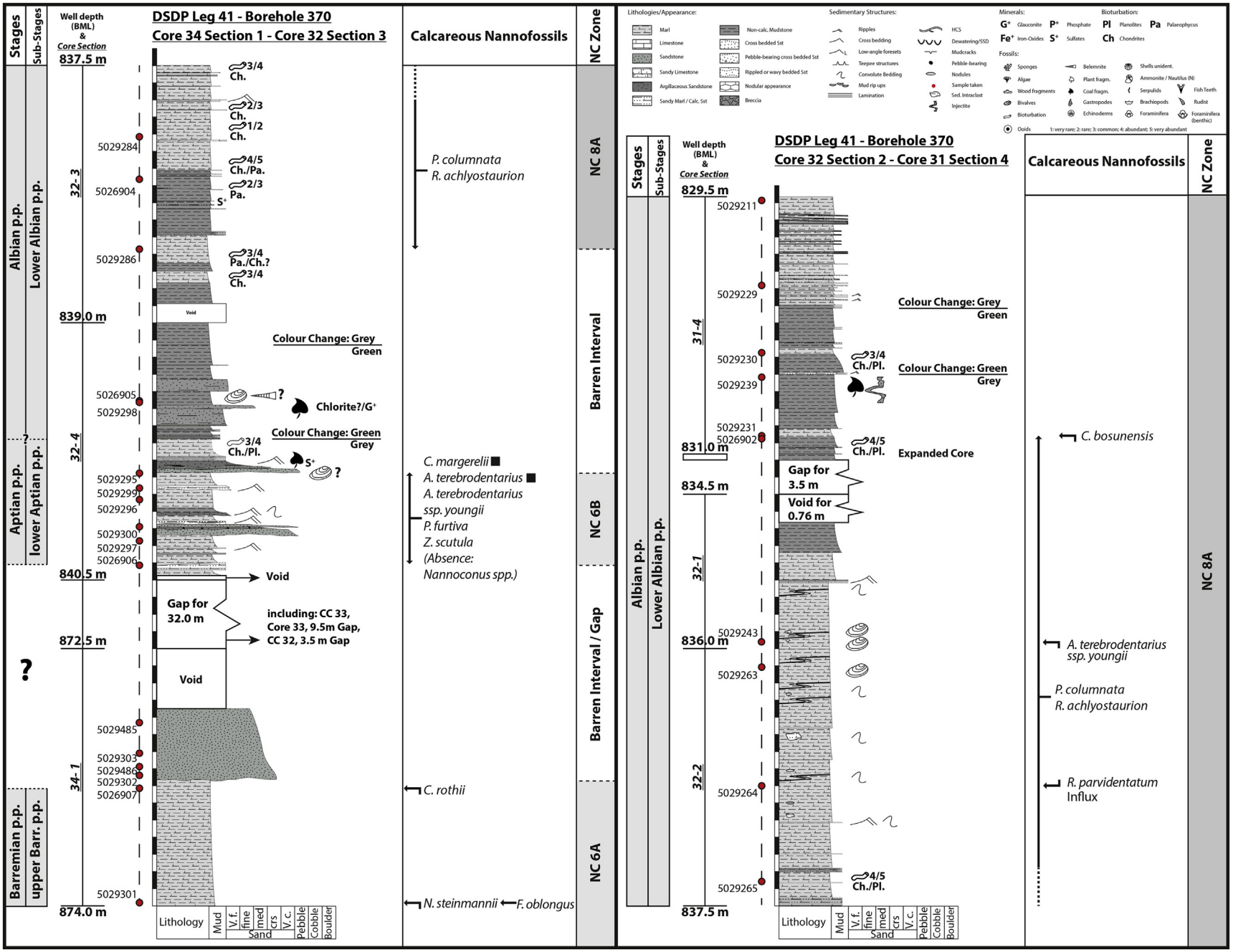

Fig. 6. DSDP borehole 370: Lithostratigraphic log and calcareous nannofossil distribution. Distribution charts for calcareous nannofossil can be found in the supplementary data.

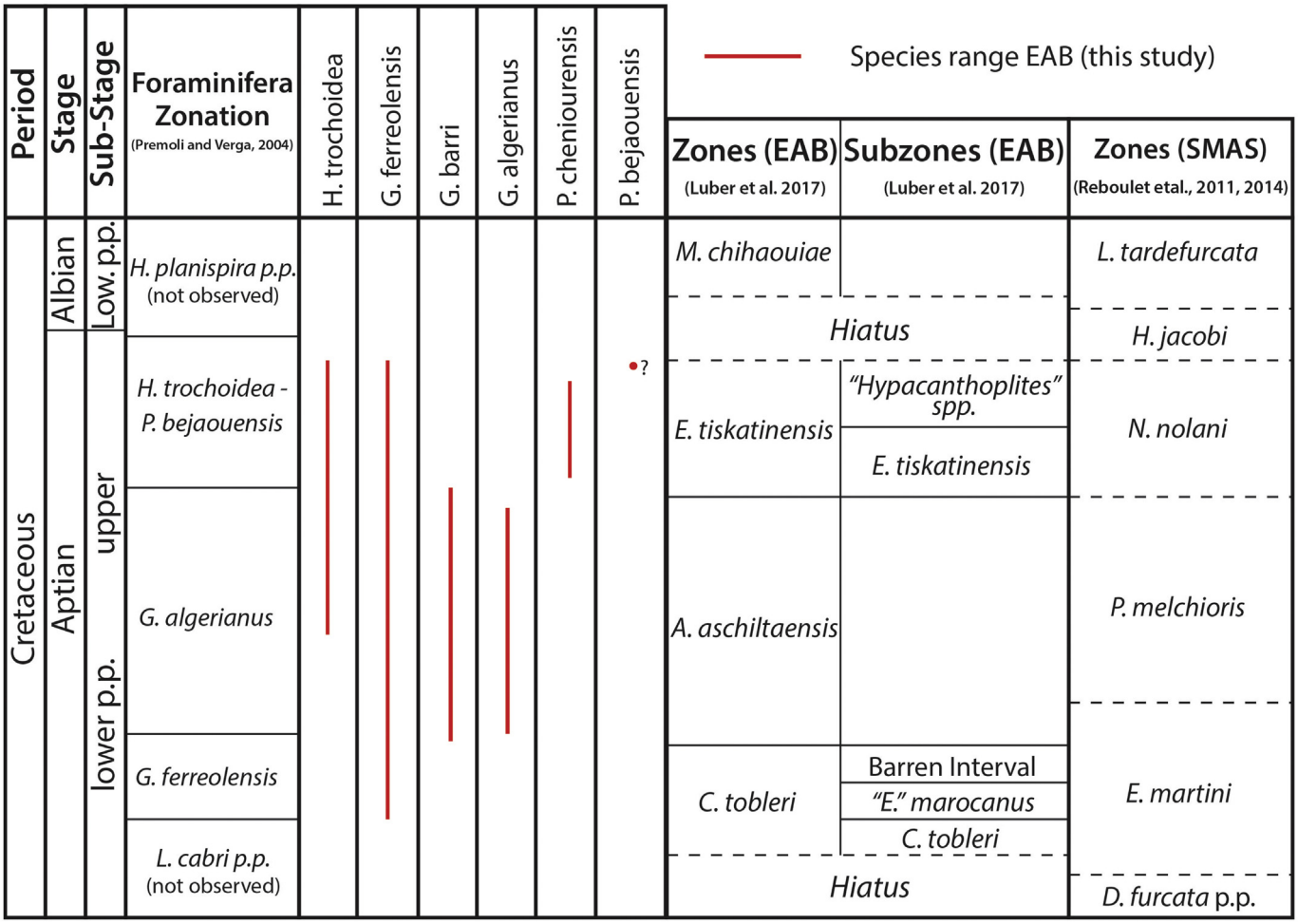

Fig. 7. Distribution of key planktonic foraminifera species and zonation (after Premoli Silva and Verga, 2004) against the local ammonoid zonation scheme in the EAB of Luber et al. (2017) and the Standard Mediterranean Ammonite Scale (SMAS) of Reboulet et al. (2011, 2014).

revision. Distribution charts for all sections are provided in the supplementary data.

3.1.3. Ammonite biostratigraphy

Bed-by-bed collections for ammonites were made from the Id Amran and Assaka section. Key bio-events were compared to the local biostratigraphic scale and bio-events of the EAB recognised by Luber et al. (2017). Key specimens are illustrated in Figs. 11 and 12.

3.2. Carbon isotope stratigraphy

75 bulk rock samples were analysed at Tiskatine. The material is almost exclusively composed of shelfal marls and limestones, with a few calcareous sandstones. The $\delta^{13}C$ analysis was performed at the Friedrich-Alexander Universität in Erlangen, Germany, using a Gasbench II connected to a ThermoFisher Delta V Plus mass spectrometer for carbonate $\delta^{13}C$ analyses and a Flash EA 2000 elemental analyser connected online to ThermoFinnigan Delta V Plus mass spectrometer for bulk organic matter $\delta^{13}C$ analyses. All values are reported in per mil relative to V-PDB. Sample preparation procedure and standards follow Bodin et al. (2017). Reproducibility for carbonate $\delta^{13}C$ was ±0.04, for $\delta^{18}O$ ±0.05, and for $\delta^{13}Corg$ ±0.07‰ (1σ).

4. Results

4.1. Biostratigraphy of the Essaouira-Agadir Basin

Herein we discuss foraminifera and calcareous nannofossils data supplementing the biostratigraphic framework of Luber et al. (2017) at the Tiskatine section and additional data from the Id Amran and Assaka sections.

4.1.1. Foraminifera biostratigraphy – zonation and key events (Tiskatine Section)

Fig. 13 shows the relative proportions of the three main types of foraminifera (agglutinating, calcareous benthic, and planktonic). Although planktonic foraminifera usually comprise the dominant component of the assemblages (50% or more of the total numbers), benthic foraminifera are also abundant and diverse. These include calcareous rotalid species and agglutinating species. Calcareous miliolids are very rare.

***Globigerinelloides ferreolensis* Zone: samples MTTK 164 – MTTK 186**

Definition: This zone was defined by Moullade (1966) as the interval from the extinction of *Leopoldina cabri* (Sigal, 1952) (=*Schackoina cabri*) to the inception of *Globigerinelloides algerianus* Cushman and Ten Dam, 1948.

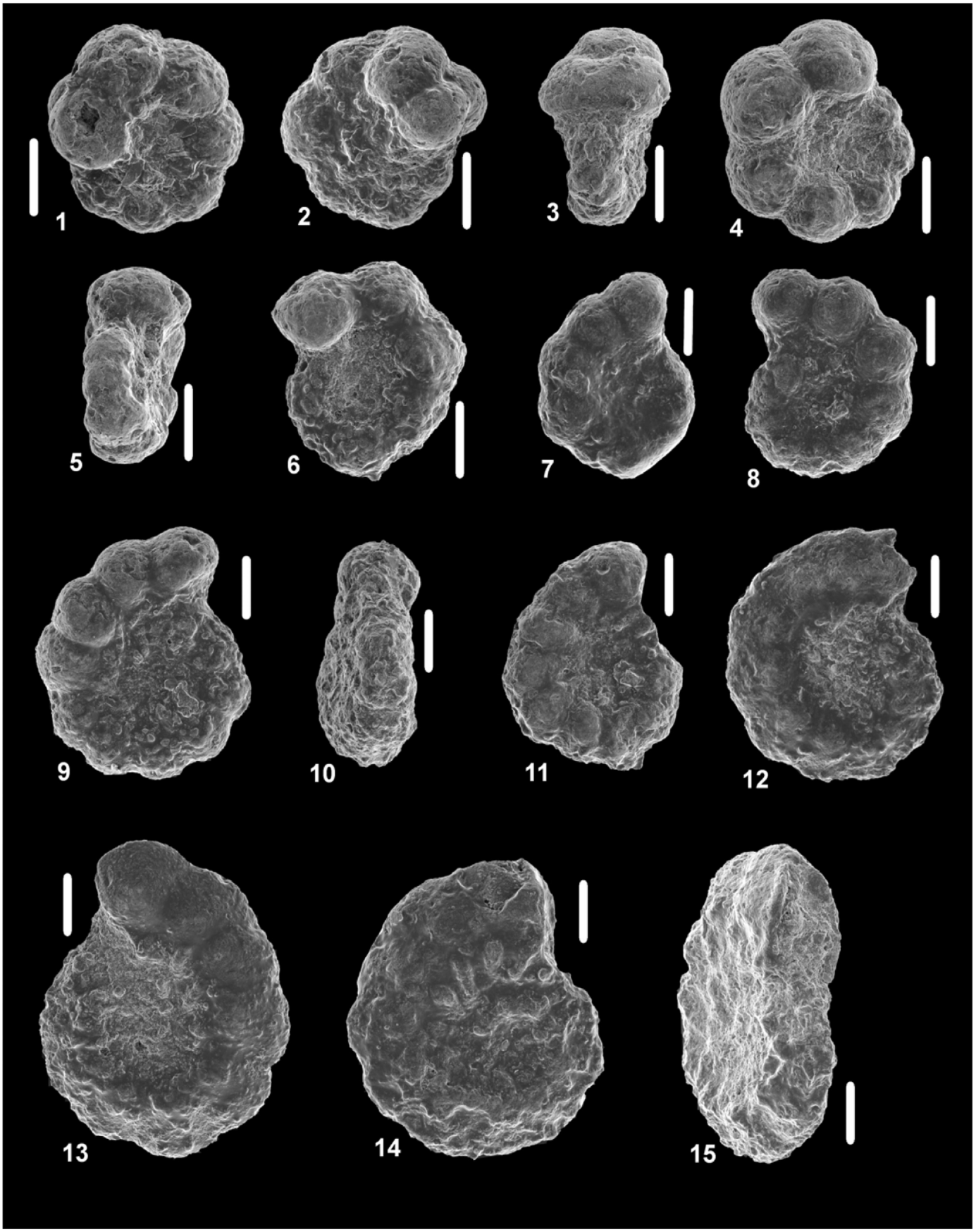

Fig. 8. Plate 1: Scanning electron microscope images of selected planktonic foraminifera from the Tiskatine section, Morocco (all scale bars = 0.1 mm): (1–3) *Globigerinelloides barri* (Bolli, Loeblich and Tappan, 1957) from **MTTK 197**; (4–6) *Globigerinelloides ferreolensis* (Bolli, Loeblich and Tappan, 1957) from **MTTK 197**; (7–8) *G. ferreolensis* - *G. algerianus* transitional form from **MTTK 185a**; (9–11) *Globigerinelloides algerianus* Cushman and Ten Dam, 1948 from **MTTK 197**; (12–13) *Pseudoplanomalina cheniourensis* (Sigal, 1952) from **MTTK 217**; (14–15) *Pseudoplanomalina cheniourensis* (Sigal, 1952) from **MTTK 237**.

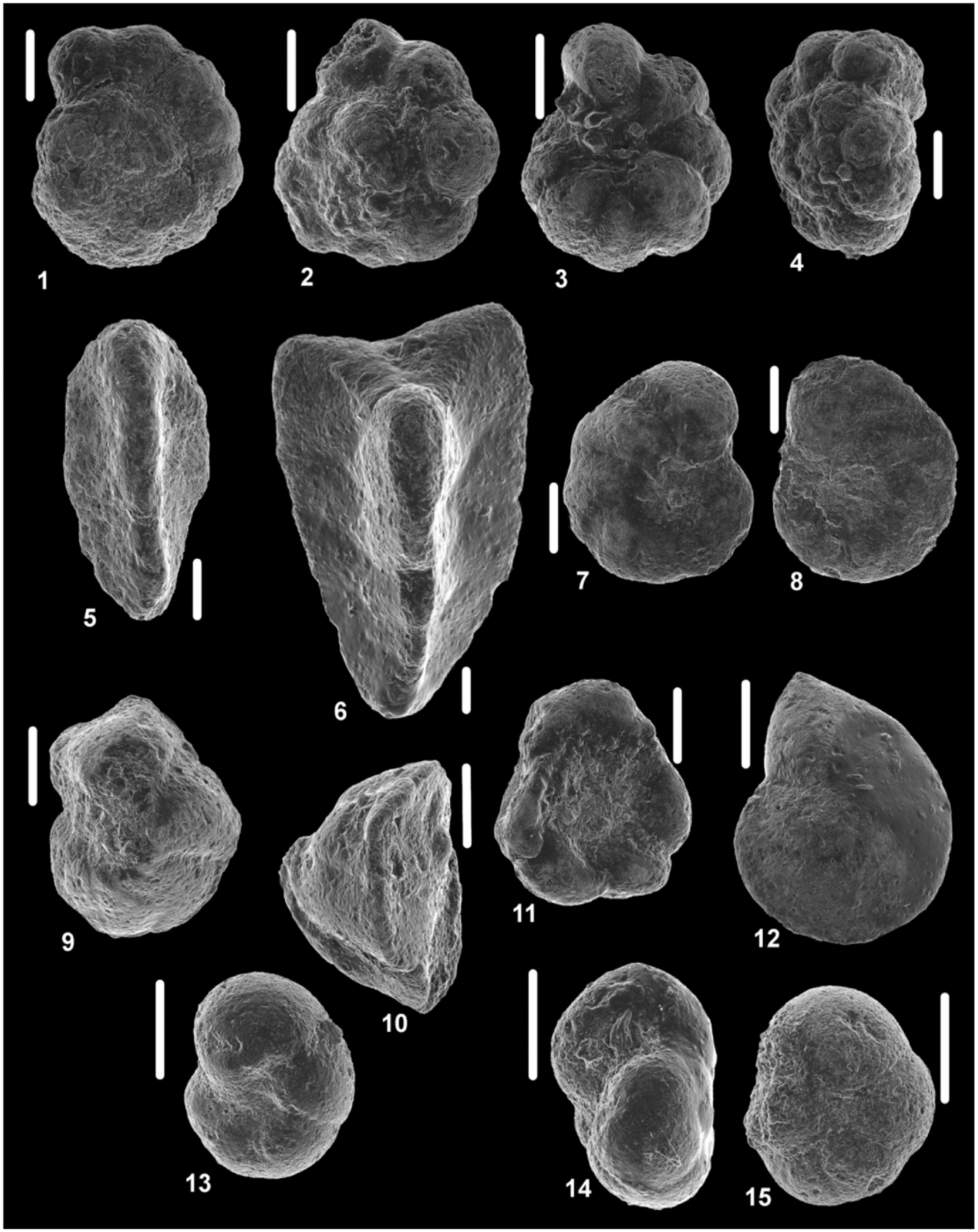

Fig. 9. Plate 2: Scanning electron microscope images of selected planktonic foraminifera from the Tiskatine section, Morocco (all scale bars = 0.1 mm): (1) ?*Paraticinella bejaouaensis* (Sigal, 1966) from **MTTK 247**; (2–4) *Hedbergella trocoidea* (Gandolfi, 1942) from **MTTK 235**; (5–6) *Tritaxia dividens* (Grabert, 1959), smaller morphotype, from **MTTK 227**; (7–8) *Gavelinella* cf. *barremiana* Bettenstaedt, 1952 from **MTTK 221**; (9–11) *Conorotalites aptiensis* (Bettenstaedt, 1952) from **MTTK 219**; (12) *Lenticulina muensteri* (Roemer, 1839) from **MTTK 215**; (13–15) *Valvulineria gracillima* Ten Dam, 1947 from **MTTK 227**.

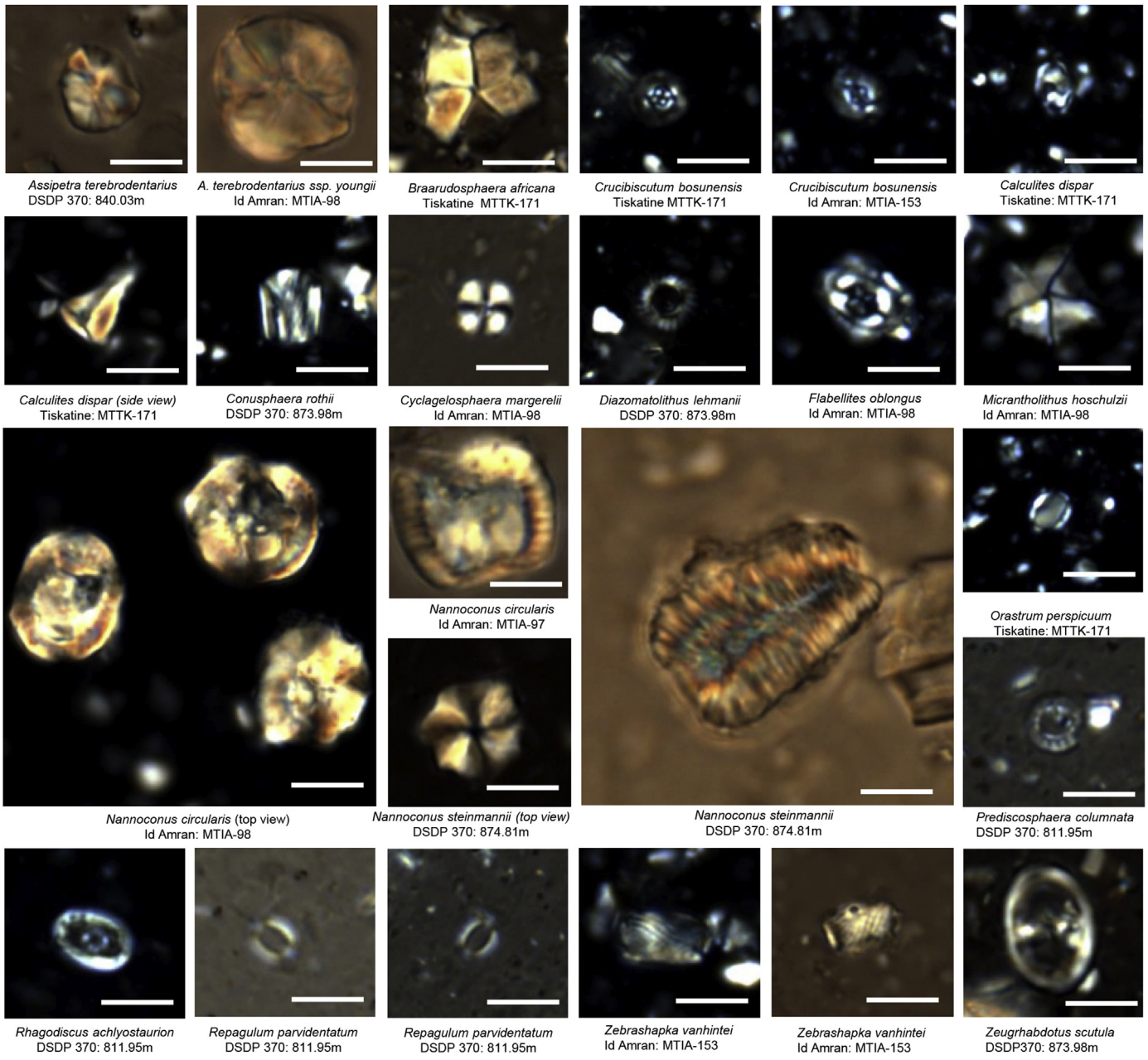

Fig. 10. Calcareous nannofossil photographic plate of key specimen from the Tiskatine and Id Amran onshore sections and DSDP borehole 370. Scale bar in all photos is = 5 μm.

Whilst rare specimens of *Globigerinelloides ferreolensis* (Moullade, 1961) can be found within the *L. cabri* Zone (Robaszynski and Caron, 1995; Verga and Premoli Silva, 2003b; Premoli Silva and Verga, 2004), extinction of *L. cabri* and the inception of common *G. ferreolensis* can be considered to be synchronous (Aguado et al., 1999; Moullade et al., 2002, 2005), so that the inception of common *G. ferreolensis* is also an effective marker for the base of the zone. At Tiskatine *G. ferreolensis* (Fig. 8.4–6) occurs almost at the base of the Tamzergout Fm. in sample **MTTK 164** (Fig. 13). The uppermost part of the zone contains forms transitional between *G. ferreolensis* and *G. algerianus* (Fig. 8.7–8) as well as specimens of *Globigerinelloides barri* (Bolli, Loeblich and Tappan, 1957).

***Globigerinelloides algerianus* Zone: samples MTTK 187 – MTTK 208**

Definition: This zone was defined by Moullade (1966) as encompassing the total range of the nominate species (Fig. 8.9–11).

This occurs between beds **MTTK 187** and **MTTK 203** at Tiskatine. The top of the zone can be extended to sample **MTTK 208** (Fig. 13) which contains *G. barri* (Fig. 8.1–3), a species that does not extend above the *G. algerianus* Zone. Although a range chart within Premoli Silva and Verga (2004) shows a minute extension of *G. barri* above the *G. algerianus* Zone, Verga and Premoli Silva (2003a) stated that "*Globigerinelloides barri* disappears at the top of the *Globigerinelloides algerianus* Zone". The local inception of

Hedbergella trocoidea (Gandolfi, 1942) occurs midway within this zone.

***Hedbergella trocoidea* – *Paraticinella bejaouensis* zones undifferentiated: samples MTTK 210 – MTTK 247**

Definition: The *Hedbergella trocoidea* Zone is, according to Sigal (1977), the interval from the extinction of *G. algerianus* to the inception of *Paraticinella bejaouensis* (Sigal, 1966). The *Paraticinella bejaouensis* Zone is defined (Robaszynski and Caron, 1995) as the total range of the nominate species.

Since *P. bejaouensis* (Fig. 9.1) does not definitely occur in our studied material (a questionable specimen occurs in sample **MTTK 247**), the interval above the *G. algerianus* Zone with planktonic foraminiferal recovery (samples **MTTK 210 – MTTK 247**) must be assigned to an undifferentiated *H. trocoidea – P. bejaouensis* zones (Figs. 7 and 13). This is supported by the presence of *Pseudoplanomalina cheniourensis* (Sigal, 1952) (Fig. 8.12–15), a species that ranges no higher than the lower part of the *P. bejaouensis* Zone (Moullade et al., 2002; Bellier and Moullade, 2002; Ando et al., 2013). Additional taxa include *G. ferreolensis* and *H. trocoidea* (Fig. 9.2–4), two species that range throughout the Upper Aptian (Moullade et al., 2002). The name *P. bejaouensis* is retained for reference to the standard literature, although proposals exist to correct the name of this species and its nominate zone to *Paraticinella rohri* (Ando et al., 2013).

4.1.2. Calcareous nannofossil biostratigraphy – zonation and key events (Tiskatine Section)

All samples analysed from the Bouzergoun Fm. proved barren of nannoplankton (**MTTK 160 – MTTK 162**). The basal 0.5 m (**MTTK 163 – MTTK 164**) mudstone section of the Tamzergout Fm. yielded low diversity and abundance assemblages. Diversity and abundance markedly increases from sample **MTTK 165b** upwards.

NC7A: samples MTTK 163 – MTTK 239

Definition: Interval from FAD of *Eprolithus floralis* (Stradner, 1962) to LAD of *M. hoschulzii* (Bralower et al., 1993).

M. hoschulzii, the marker for NC7A is found sporadically throughout the Tamzergout Formation. **MTTK 239** (Fig. 13) is likely an artificial top due to the sporadic local range. A boreal marker, *Crucibiscutum bosunensis* Jeremiah, 2001 is recorded from the Tiskatine section. Its FO at Tiskatine is recorded from bed **MTTK 185b**. The acme of *C. bosunensis* is at bed **MTTK 239**. *Zebrashapka vanhintei* Covington and Wise, 1987 is found throughout the Upper Aptian but does not range up into the Lower Albian. *Assipetra terebrodentarius youngii* Tremolada and Erba, 2002 is found sporadically throughout the Tiskatine section.

Holococcoliths are particularly prevalent in the Aptian Tiskatine section. In the lower beds (**MTTK 165b – MTTK 185a**) *Calculites dispar* Varol *in* Al-Rifaiy et al., 1990 (Fig. 10) predominates. From bed **MTTK 187** above *Orastrum perspicuum* Varol *in* Al-Rifaiy et al., 1990 (Fig. 10) dominates with *Owenia partitum* (Varol *in* Al-Rifaiy et al., 1990) also showing quantitative influxes between beds **MTTK 200** and **MTTK 218**.

NC8A: sample MTTK 249

Definition: Interval from FAD of *P. columnata* to FAD of *H. albiensis* (Bralower et al., 1993).

Sample **MTTK 249** yields both the FO of NC8A marker *P. columnata* together with *Rhagodiscus achlyostaurion* (Hill, 1976) and records a quantitative acme of the predominantly boreal species *Repagulum parvidentatum* (Deflandre and Fert, 1954) (Fig. 10). Holococcoliths and nannoconids are rare compared to the underlying Upper Aptian, diversity and abundance of the nannofloras reduced.

4.1.3. Ammonite biostratigraphy (Id Amran Section)

Compared to the biostratigraphic framework of Luber et al. (2017) the following ammonoid bio-events are recognised:

- Bio-event 1: occurrence of *Prochelonicerasdechauxi* (Kilian and Reboul, 1915) in **MTIA 84**
- Bio-event 2: peak of diversity dominated by *Colombiceras* and *Epicheloniceras* **MTIA 105**
- Bio-event 3: first occurrence (FO) of the endemic species "*Epicheloniceras*" *marocanus* (Roch, 1930) in **MTIA 106**
- Bio-event 5: peak of abundance of *Pseudoaustraliceras* in beds **MTIA 131** and **135**
- Bio-event 6: sudden mass occurrence of *Elsaisabellia* in bed **MTIA 15**

Two additional ammonoid faunas are recognized by comparison to the ammonoid succession at Tiskatine. In bed **MTIA 98** the assemblage is dominated by "*Prochelonicerasn*" sp. nov. (Fig. 11.11–17), large ancyloceratids associated with *Deshayesites* aff. *callidiscus* Casey, 1961a (Fig. 11.1–2). Slightly above bed **MTIA 100** contains an abundant fauna dominated by *Dufrenoyia praedufrenoyi* Casey, 1964 *sensu* Dutour (2005) (Fig. 11.3–9) and the occurrence of *Toxoceratoides rochi* Casey, 1961b (Fig. 11.10) is noteworthy.

4.1.4. Calcareous nannofossil biostratigraphy (Id Amran Section)

NC6B: samples MTIA 89 – MTIA 95

The lowermost Aptian nannofloras (**MTIA 89 – 95**) investigated from Id Amran are extremely rich yielding *Diazomatolithus lehmanii* Noël, 1965 (Fig. 10), high relative abundances of *Cyclagelosphaera margerelii* Noël, 1965 (Fig. 10) and *Assipetra terebrodentarius* (Applegate et al. in Covington and Wise, 1987) (Fig. 10), events all occurring below the FAD of *E. floralis*. At Id Amran a rich nannoconid association also occurs with the wide canal forms *Nannoconus circularis* Deres and Achéritéguy, 1980 (Fig. 10) and *Nannoconus vocontiensis* Deres and Achéritéguy, 1980 predominant. The assemblage in this interval indicates zone NC6B.

The *D. forbesi* zone dated deposits at Id Amran between **MTIA 89** and **MTIA 95** are stratigraphically younger than the deposits immediately below the basal Albian unconformity at DSDP 370 and 416A (see below). At DSPD 370 the samples also yield *Zeugrhabdotus scutula* (Bergen, 1994) (Fig. 10) a form characteristic of the lower part of zone NC6B (Fig. 6).

NC7A: samples MTIA 104 – MTIA 151

MTIA 104 yields the FAD of *E. floralis* together with the LAD of *N. circularis*. Additional events include the occurrence of *C. bosunensis* and *M. hoschulzii* recorded from, **MTIA 151** and **MTIA 153** (*E. tiskatinensis* Zone). Additionally, **MTIA 153** yielded common *C. bosunensis* and an incursion of common *Z. vanhintei* (Fig. 10) *(E. tiskatinensis* Zone).

NC8A: sample MTIA 156

P. columnata, *R. achlyostaurion* and rare *C. bosunensis* are recorded from **MTIA 156**, confirming a basal Albian age (NC8A).

4.1.5. Ammonite biostratigraphy (Assaka Section)

The co-occurrence of *Epicheloniceras* and *Colombiceras* in **MTAS 121** indicates the Lower Upper Aptian *C. tobleri* Zone and Subzone. The mass occurrence of *Epicheloniceras* in **MTAS 122** suggests a similar age, even though the occurrence of elements from the "*E.*" *marocanus* Subzone cannot be excluded. The fauna collected from **MTAS 123** contains reworked Upper Aptian ammonites from the *A. aschiltaensis* Zone [*Pseudoaustraliceras* gr. *ramososeptatum* (Anthula, 1900)], from the *E. tiskatinensis* Zone ["*Epicheloniceras*" gr.

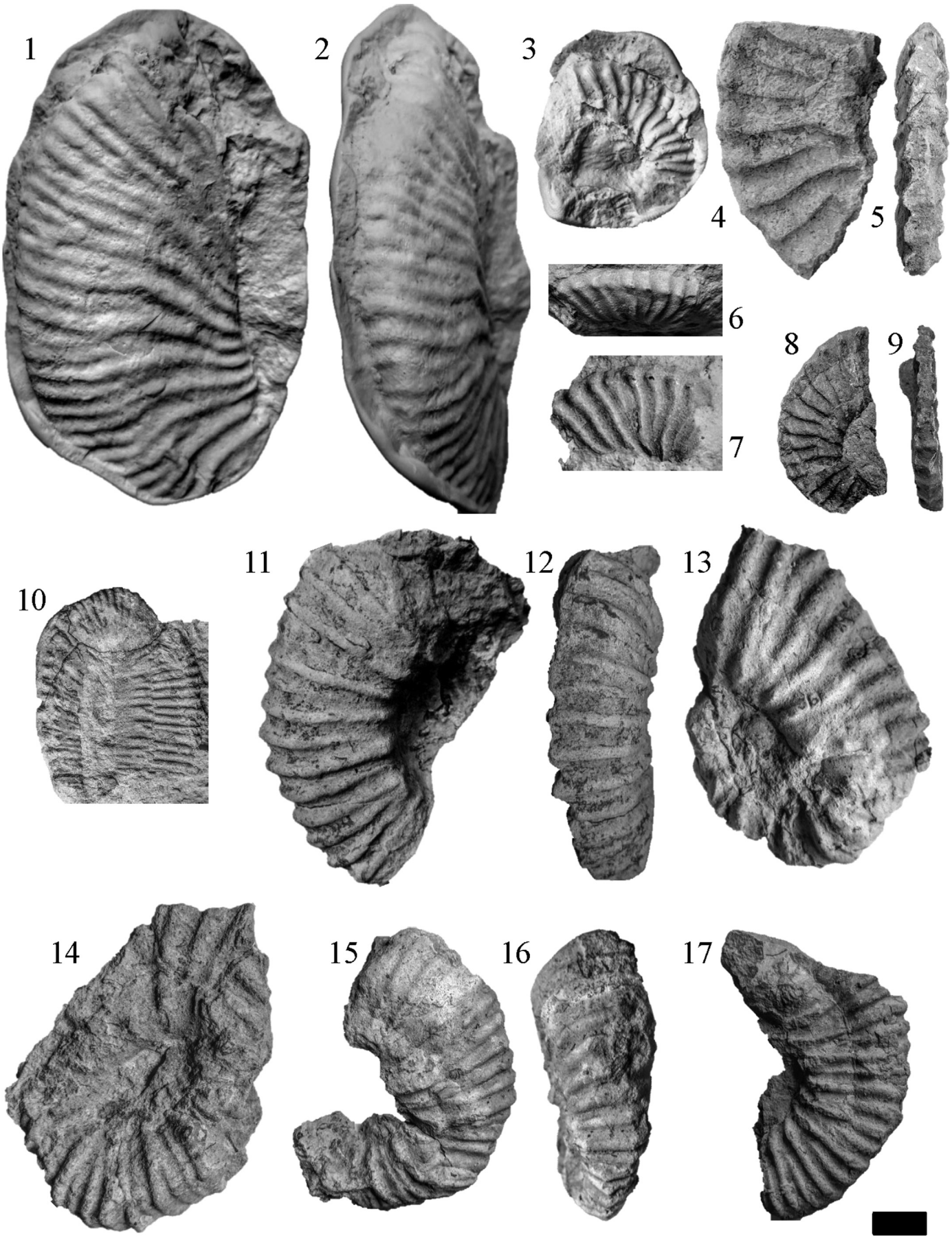
1
2
3
4
5
6
7
8
9
10
11
12
13
14
15
16
17

clansayense (Jacob, 1905)] together with *Mellegueiceras* and "*Hypacanthoplites*" of the *paucicostatus* (Breistroffer in Dubourdieu, 1953) group that are diagnostic of the Lower Albian (Latil, 2011; Luber et al., 2017). Key ammonoid material is illustrated in Fig. 12.

4.1.6. Calcareous nannofossil biostratigraphy (Assaka Section)

NC8A: sample MTAS 124

An Early Albian age for **MTAS 124** is established by the co-occurrence of *P. columnata* and a questionable specimen of *R. achlyostaurion*.

4.1.7. Nannofossil biostratigraphy DSDP Leg 41 borehole 370

The following key bio-events have been recognised in the studied section (Fig. 6):

NC6A

- 1. LO of common nannoconids and *Micrantholithus obtusus* Stradner, 1963; presence of *Flabellites oblongus* (Bukry, 1969) (Fig. 10) at 874.81 m indicating an age no older than latest Barremian (Zone NC6A).
- 2: *LO of Nannoconus steinmannii* Kamptner, 1931 (Fig. 10) at 873.98 m
- 3: LO of *Conusphaera rothii* (Thierstein, 1971) (Fig. 10) at 873.31 m. In this study the LAD of *C. rothii* is utilised as an approximation for top Barremian (Zone NC6A).

NC6B

- 4. LO of *Z. scutula* at 840.03 indicating an age no younger than earliest Aptian (Zone NC6B).
- 5: LO of HRA of *C. margerelii* with an influx of *A. terebrodentarius* and LO of consistent *P. furtiva* in the absence of *E. floralis* indicating an age no younger than Early Aptian intra *D. forbesi* ammonite Zone equivalent age at 839.87 m (Zone NC6B).

NC8A

- 6. FO of *R. achlyostaurion*, presence of *C. bosunensis* and *A. terebrodentarius youngii* indicates a basal Albian age at 838.57 m (Zone NC8A).
- 7. FO of *P. columnata* at 837.90 m (Zone NC8A).
- 8. LO of *A. terebrodentarius youngii* at 835.95 m (Zone NC8A). *A. terebrodentarius youngii* is more extensively recorded from the oceanic DSDP 370 than at the shallower shelf outcrop at Tiskatine, a result of this form's preference to deeper waters (Street and Bown, 2000).
- 9. FO of an influx of *R. parvidentatum* at 836.80 m.
- 10. LO of *C. bosunensis* at 830.89 m (Zone NC8A).
- *C. bosunensis* is found from 830.89 m down to the basal Albian sample analysed at 838.57 m.

At the DSDP 370 borehole both *C. bosunensis* and *A. terebrodentarius youngii* are found to have LO's extending into the basal Albian.

4.1.8. Nannofossil biostratigraphy DSDP Leg 41 borehole 416

The following key bio-events have been recorded in core 6-4 and 6 core catcher (CC):

- Lowermost Aptian deposits yielding abundant *A. terebrodentarius*, common *C. margerelii* and common *Z. scutula*, again in the absence of nannoconids (core 6 CC); lower part Zone NC6B.
- Lower Albian deposits yielding an influx of *R. parvidentatum*, abundant *R. achlyostaurion* and the presence of *P. columnata* (core 6 CC and 6-4); Zone NC8A.

4.2. Carbon isotope stratigraphy: $\delta^{13}C_{carb}$ and $\delta^{13}C_{org}$

The $\delta^{13}C_{carb}$ values of the Tiskatine section between **MTTK 163** and **MTTK 249** (Fig. 14) range between −0.34‰ (**MTTK 249**) and 1.9‰ (**MTTK 229**) and can be grouped into 5 major segments.

- **Segment 1**: Overall increase of $\delta^{13}C_{carb}$ values from −0.13‰ to 1.83‰ between **MTTK 163** to **MTTK 172**, with wide scatter of values between **MTTK 163** to **MTTK 169.**
- **Segment 2**: Decreasing trend of $\delta^{13}C_{carb}$ values following **MTTK 172** to 0.31‰ in **MTTK 185b.**
- **Segment 3**: Overall plateau of $\delta^{13}C_{carb}$ values from **MTTK 186** to **MTTK 206/208**, oscillating between 0.29 (**MTTK 197**) and 1.32‰ (**MTTK 204**). A small long-term increasing trend can be observed within the segment. On top of segment 3, a short-lived negative excursion (from **MTTK 206** to **MTTK 213**) can be observed.
- **Segment 4**: Rapid increasing trend in $\delta^{13}C_{carb}$ values from **MTTK 213** to **MTTK 216** followed by an attenuated increase towards a maximum value in the section of 1.90‰ in **MTTK 229.**
- **Segment 5**: Pronounced decreasing trend of $\delta^{13}C_{carb}$ values following **MTTK 229** to the minimum value in the section of −0.34‰ in **MTTK 249.**

The $\delta^{13}C_{org}$ values of the Tiskatine section between **MTTK 160** and **MTTK 249** (Fig. 14) range between −27.27‰ (**MTTK 160**) and −22.49‰ (**MTTK 161**) and can be grouped into 4 major segments.

- **Segment 1**: Decreasing trend of $\delta^{13}C_{org}$ values from **MTTK 161** (−22.49‰) to −26.86‰ in **MTTK 186.**
- **Segment 2**: Overall plateau of $\delta^{13}C_{org}$ values from **MTTK 186** to **MTTK 206** (−26.5‰).
- **Segment 3**: Increasing values until **MTTK 226** (−25.21‰).
- **Segment 4**: Overall plateau until the basal Albian unconformity.

5. Discussion

5.1. Biostratigraphy

5.1.1. Age interpretation foraminifera

All planktonic foraminifera present suggest a Late Aptian age for the Tamzergout Fm. at Tiskatine (Fig. 7). Early Aptian taxa, such as the distinctive *L. cabri*, are absent and the lowest significant planktonic foraminifera occurring in the section, *G. ferreolensis*, is restricted to the Late Aptian according to some authors (e.g. Moullade et al., 2002). The occurrence of this species in the highest part of the Tamzergout Fm. (Fig. 13) indicates a Late Aptian age (along with the presence of *H. trocoidea* and, just below these occurrences, *P. cheniourensis*) (Premoli Silva and Verga, 2004). Taxa indicative of an Early Albian age such as *T. primula* are absent from the Tamzergout Fm. at Tiskatine. Ammonoid and calcareous nannofossil occurrences demonstrate an Albian age for the overlying Oued Tidzi Fm. This interpretation

Fig. 11. Ammonoid photographic plate of the Id Amran section (scale bar = 1 cm): (1–2) *Deshayesites* aff. *callidiscus* Casey, 1961a from bed **MTIA 98** ((Manch) LL. 16142); (3–9) *Dufrenoyia praedufrenoyi* Casey, 1964 from bed **MTIA 100** ((Manch) LL. 16144); (10) *Toxoceratoides rochi* Casey, 1961b from bed **MTIA 100** ((Manch) LL. 16145); (11–17) "*Prochelonicera*" sp. nov. from bed **MTIA 98** ((Manch) LL. 16143).

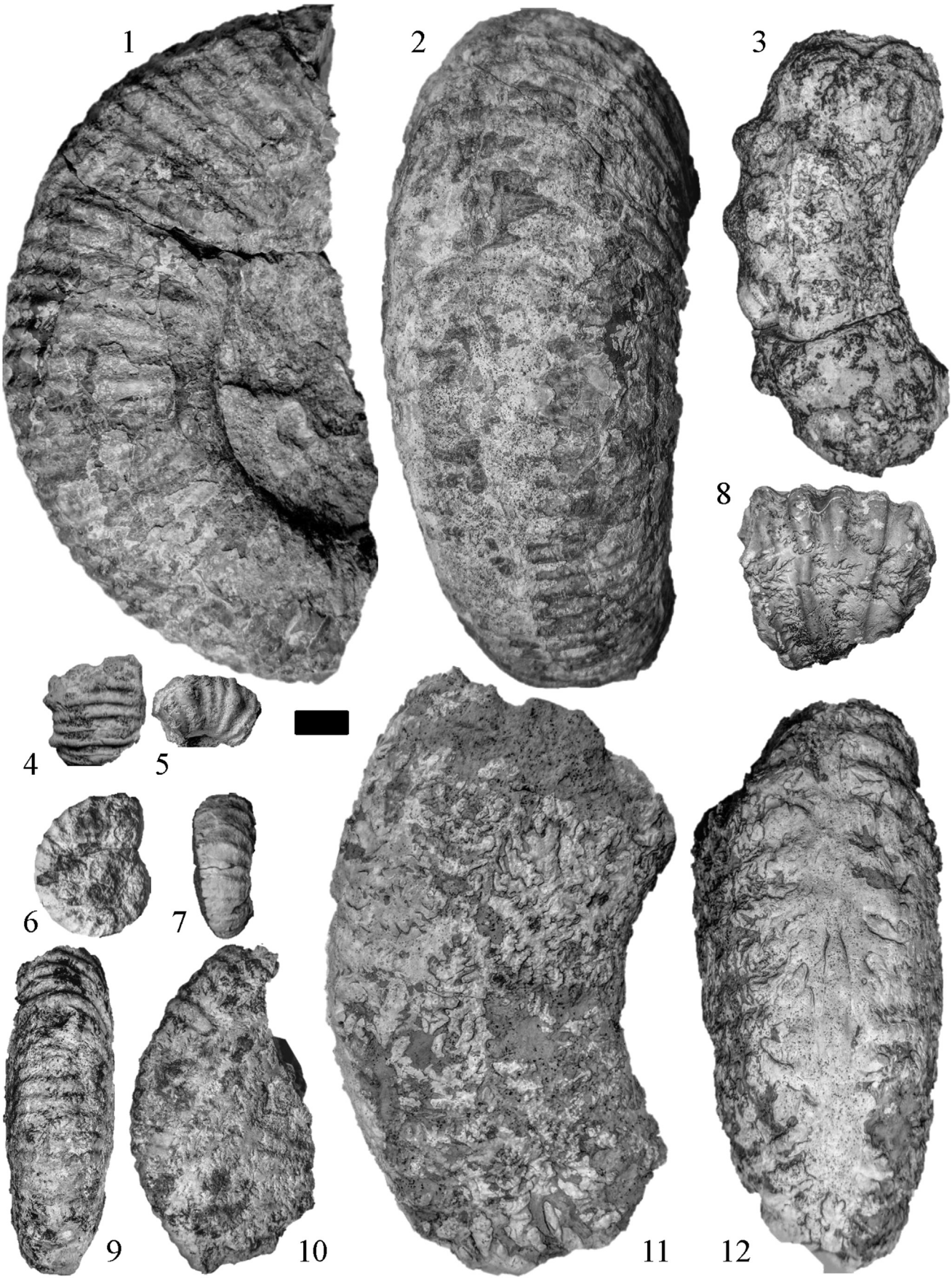
1
2
3
8
4
5
6
7
9
10
11
12

contrasts with that of Yamina et al. (2002) who described, but did not illustrate, a variety of Early Aptian planktonic foraminiferas species from the lower part of the Tamzergout Fm. at localities north of the Amsittene Anticline. The ammonoid work of Luber et al. (2017) highlighted that the base of the Tamzergout Fm., as originally defined by Duffaud et al. (1966) is markedly diachronous being the lower part of the Lower Aptian at some localities and Lower Upper Aptian at others (Fig. 2). A possibility to explain the discrepancies in age interpretation, in addition to the difficulties in applying lithostratigraphy, is that the Tiskatine section represents deposition in proximity of a local high, such that the well-established intra-Aptian hiatus (sequence boundary) (Peybernes et al., 2013; Luber et al., 2017) is most expansive there.

The Late Aptian age interpretation of the Tamzergout Fm. at Tiskatine provided by the planktonic foraminifera is in broad agreement with the age interpretations provided here from the occurrences of ammonoids and calcareous nannofossils (Fig. 13), as well as the stable carbon isotope record (Fig. 14). It is very likely that the uppermost Aptian "*H*". *jacobi* Zone is missing in the Tiskatine section as *P. cheniourensis* occurs near the top of the formation, a species with a LAD well below the top of the Aptian or reported "uppermost Gargasian" (Moullade et al., 2002; Ando et al., 2013). Ammonoid, calcareous nannofossils, and carbon isotope records support this interpretation (Figs. 13 and 14).

The calibration of the standard planktonic foraminiferal zonation to the SMAS is still in progress as, regrettably, a limited number of publications document the co-occurrence of planktonic foraminifera alongside ammonoid occurrences in the classic sections. The data from the Tiskatine section may be very important in this respect as the local ammonoid zonation of Luber et al. (2017) can be calibrated to the SMAS and the $\delta^{13}C$ record. Calcareous nannofossils provide additional constraint.

The oldest ammonites found in the Tamzergout Fm. at Tiskatine are assigned to the *C. tobleri* Zone. This is calibrated to a position midway within the *E. martini* Zone of the SMAS (Luber et al., 2017). The recognition of the *G. ferreolensis* planktonic foraminiferal Zone for the same samples is intriguing in that for some authors the *G. ferreolensis* Zone is regarded as occurring at the base of the Upper Aptian, in the lowest part of the *E. martini* Zone (Ogg and Hinnov, 2012). Our data would suggest that positioning the base of *G. ferreolensis* Zone above the base of the Upper Aptian, within the *E. martini* Zone (Figs. 7 and 13) would be preferable as indicated by Robaszynski and Caron (1995) and Dauphin (2002). The $\delta^{13}C$ record points to calibration with the Ap9 segment of the standard $\delta^{13}C$ curve from the Vocontian Trough. Ap9 is low within the *E. martini* Zone and calibrates with the *G. ferreolensis* Zone.

The local *A. aschiltaensis* ammonite Zone found in the middle part of the Tamzergout Fm. at Tiskatine is calibrated (Luber et al., 2017) to straddling the upper *E. martini* to *P. melchioris* zones of the SMAS. The portion of the Tiskatine section assigned to the *A. aschiltaensis* Zone is also assigned to the *G. algerianus* planktonic foraminifera Zone and the upper part of the *G. ferreolensis* Zone. Although these zones are calibrated by some authors to levels within the *E. martini* Zone (e.g. Ogg and Hinnov, 2012) the data from Tiskatine (Fig. 13) would suggest that placement of the top of the *G. algerianus* Zone extends to the *P. melchioris* Zone as suggested by Robaszynski and Caron (1995) and Dauphin (2002).

5.1.2. Age interpretation ammonites and biostratigraphic correlation to the Standard Mediterranean Ammonite Scale (SMAS)

A state of the art of the integrated ammonoid, planktonic foraminifera, and calcareous nannofossil distribution in the reference sections of the South Provence and Vocontian basins are presented in the supplementary data. These synthetic figures include both published (Bergen, 2000; Kennedy et al., 2000, 2014; Moullade et al., 2000, 2005; Dauphin, 2002; Herrle and Mutterlose, 2003; Dutour, 2005; Kuhnt and Moullade, 2007; Frau et al., 2015) and unpublished data by two of us (CF and LGB). The bio-events selected are the ones more reliable to correlate the EAB and the SMAS successions (Luber et al., 2017). Formal revision of the SMAS is far beyond the scope of the present contribution. This work is currently in progress and will be published elsewhere.

As outlined by Luber et al. (2017) the lack of precise definition of the Aptian and Lower Albian biochronozones and subzones of the SMAS handicaps the correlation between the EAB and the SMAS. This point was already addressed by Owen (1996), Dauphin (2002), Bulot (2010), Bulot et al. (2014), Frau et al. (2015, 2016). Consequently, the high-resolution integrated stratigraphy of the Aptian stage is at a far more preliminary stage than advocated (see also discussions in Frau et al., 2018).

Id Amran

By comparison with the ammonoid successions of SE France the fauna from **MTIA 98** indicates the middle part of the *D. forbesi* Zone *sensu* Frau et al. (2015). The assemblage from **MTIA 100** is indicative of the middle part of the *D. furcata* Zone *sensu* Dutour (2005). Therefore, these two Early Aptian ages demonstrate the existence of a hiatus that spans the upper part of the *D. forbesi* Zone, the *D. deshayesi* Zone and the lower part of the *D. furcata* Zone on top of bed **MTIA 98**. The hiatus includes the time equivalent of the OAE 1a-related culmination and succeeding recovery. These ages are further supported by the occurrence of the calcareous nannofossil association of *E. floralis* and *N. circularis* in **MTIA 104** of latest Early Aptian age.

5.1.3. Age interpretation calcareous nannofossils

Tiskatine

NC7A: The LAD of *M. hoschulzii* has been conventionally calibrated (Bralower et al., 1993; Ogg and Hinnov, 2012) to a position slightly above the base of the Upper Aptian, at a level close to the base of the *E. martini* Zone (SMAS). This conventional calibration for the top NC7A appears depressed to more recent records from northwestern Europe (Jeremiah, 2000, 2001), the Gulf of Mexico (Phelps et al., 2015; Supplementary document) and this study at Tiskatine (EAB). Here at Tiskatine *M. hoschulzii* ranges up to the local "*Hypacanthoplites*" spp. Subzone, correlated to the upper part of the *A. nolani* Zone (Fig. 13). It is uncertain whether its LO at **MTTK 239** is its true LAD, or a result of truncation at the Aptian/Albian boundary unconformity above (Fig. 13). Regardless, the range of *M. hoschulzii* substantially extends the conventional LAD.

The occurrence of the boreal marker *C. bosunensis* is noteworthy at Tiskatine and could help establish a calibration datum between the Boreal and Tethyan realms. In the boreal North Sea, *C. bosunensis* has a short stratigraphic acme range constrained to the uppermost beds of the *E. martinoides* and *P. nutfieldensis* zones of Early Late Aptian age (Jeremiah, 2000). Its true LAD is more

Fig. 12. Ammonoid photographic plate of the Assaka section (scale bar = 1 cm): (1–2) *Epicheloniceras* gr. *waageni* (Anthula, 1900) – *tschernyschewi* (Sinzow, 1906) from bed **MTAS 122** ((Manch) LL. 16147); (3) *Pseudoaustraliceras* gr. *ramososeptatum* (Anthula, 1900) from bed **MTAS 123** ((Manch) LL. 16149); (4–5) *Epicheloniceras* gr. *gracile* Casey, 1961a from bed **MTAS 121** ((Manch) LL. 16146); (6–7) *Epicheloniceras* gr. *subbuxtorfi* – *paucinodum* (Burckhardt, 1925) from bed **MTAS 122** ((Manch) LL. 16148); (8) "*Hypacanthoplites*" cf. *paucicostatus* (Breistroffer *in* Dubourdieu, 1953) from bed **MTAS 123** ((Manch) LL. 16150); (9–10) *Mellegueiceras* cf. *chihaouiae* Latil, 2011 from bed **MTAS 123** ((Manch) LL. 16151); (11–12) *Pseudoaustraliceras* gr. *ramososeptatum* (Anthula, 1900) from bed **MTAS 123** ((Manch) LL. 16152).

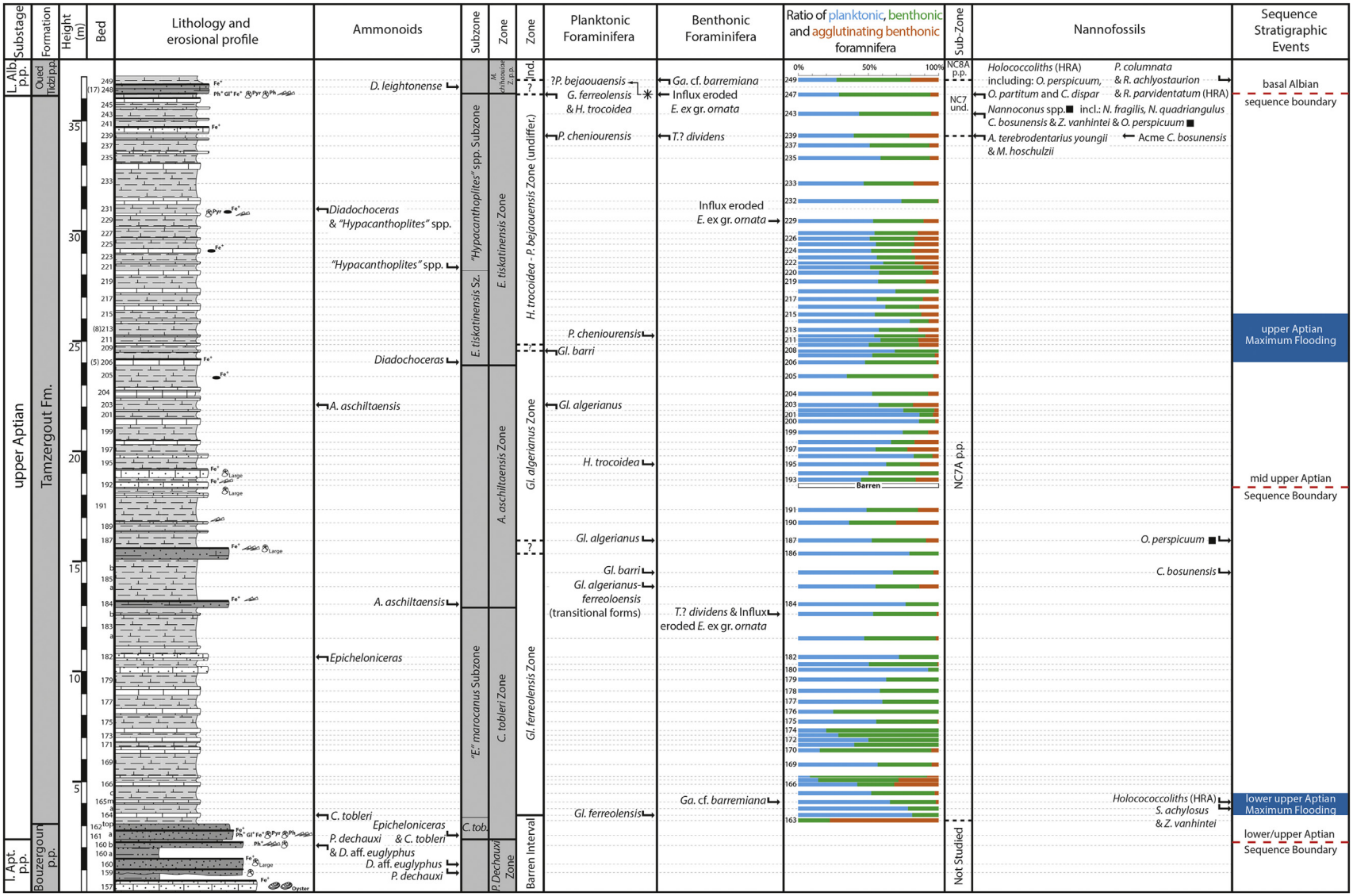

Fig. 13. Integrated biostratigraphic chart of the Tiskatine section, EAB. Local ammonoid zonation scheme of Luber et al. (2017), foraminifera zonation after Premoli Silva and Verga (2004) and calcareous nannofossil zonation after Roth (1978) and Bralower et al. (1993). Distribution charts for foraminifera and calcareous nannofossil can be found in the supplementary data.

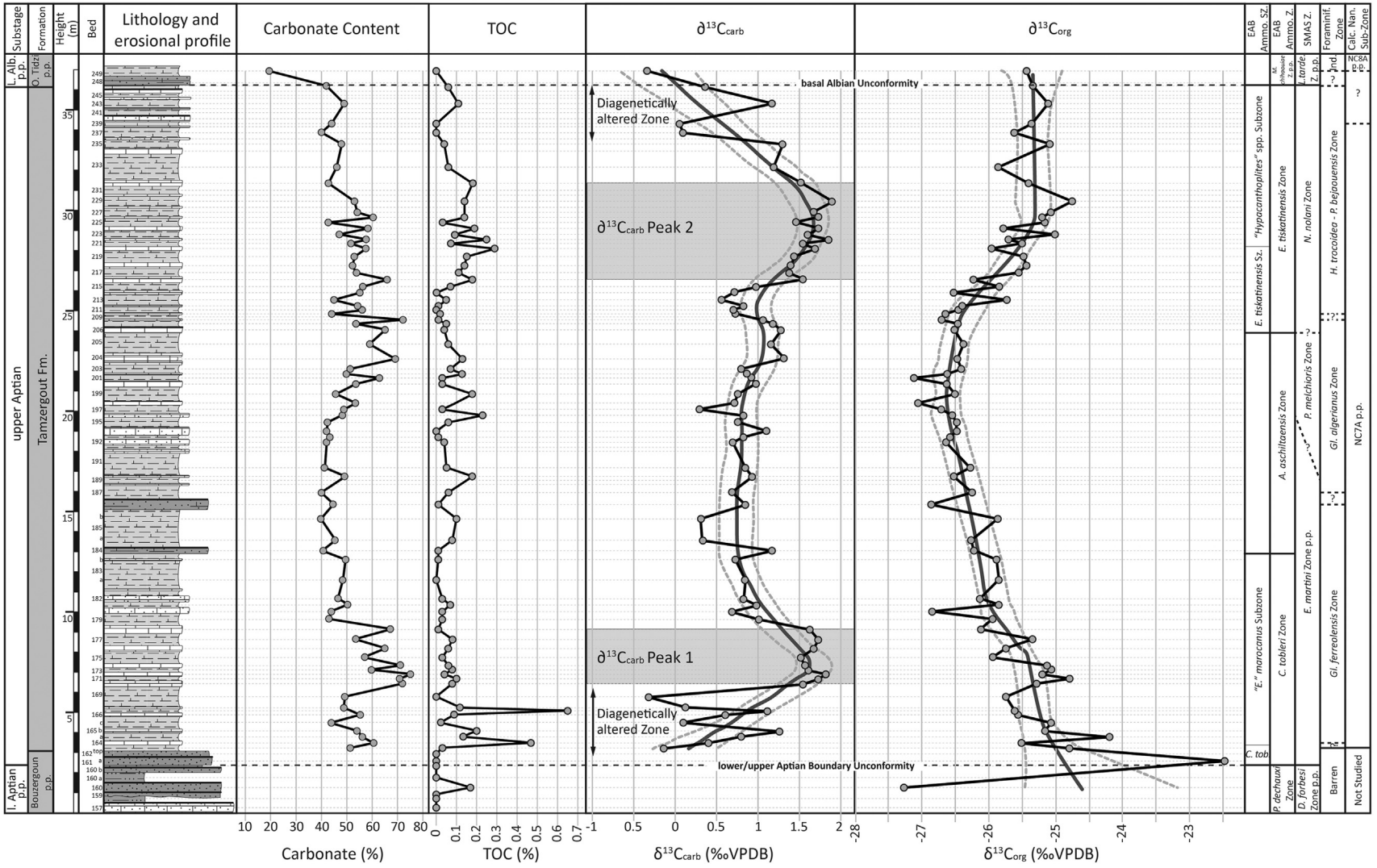

Fig. 14. Carbonate content, total organic carbon (TOC), $\delta^{13}C_{carb}$ and $\delta^{13}C_{org}$ (‰ VDPB) of the Lower Aptian to Lower Albian at Tiskatine, EAB. Findings are referenced against the local ammonoid zonation scheme in the EAB of Luber et al. (2017), the Standard Mediterranean Ammonite Scale (SMAS) of Reboulet et al. (2011, 2014), standard planktonic foraminiferal zonation of Premoli Silva and Verga (2004) and Lower Cretaceous NC Zones of Roth (1978, 1983) and subzones after Bralower et al. (1993).

sporadic, with rare occurrences ranging up into the lowermost Albian of the North Sea (Jeremiah, 2001). Recent studies (Phelps et al., 2015; supplementary document) have shown a more extensive geographical distribution outside of the North Sea. At Tiskatine the acme of *C. bosunensis* is at bed **MTTK 239** (Fig. 13). This acme only 2 m below the Aptian/Albian boundary unconformity suggests that sedimentary deposits equivalent to the uppermost Aptian *H. jacobi* Zone are extremely condensed or eroded. In the North Sea, *C. bosunensis* is only recorded rarely from *H. jacobi* dated strata (Jeremiah, 2001; Jeremiah et al., 2010).

Further, it is noteworthy that the occurrence of *Z. vanhintei* in Upper Aptian deposits (Fig. 13) extends the range of this form from its published LAD in the Lower Aptian (Bown et al., 1998).

NC7B/NC7C: Subzones NC7B and NC7C are not utilised in the current study. These subzones are based on a differentiation of the FAD of *R. achlyostaurion* from that of the FAD of *P. columnata*. Current studies indicate that the base of *R. achlyostaurion* lies close to the base of the Albian where it appears together with *P. columnata* (Kennedy et al., 2000, 2014) as at Tiskatine (Fig. 13).

NC8A: There is a major nannofloral turnover at the Aptian/Albian boundary section at Tiskatine. The FO of abundant *R. parvidentatum* is a potentially important local correlative event marking the base of the Albian along the Moroccan Atlantic Margin, here occurring with the FAD of *R. achlyostaurion* and *P. columnata* (Sample **MTTK 249**).

Id Amran

NC6B: Here the assemblage of **MTIA 89-95** is characteristic of other Lower *D. forbesi* Zone ammonite dated assemblages (Atherfield Clay, UK, Fischschiefer UK North Sea; Jeremiah, 2000; Jeremiah et al., 2010; Lehmann et al., 2012, 2016).

NC7A: Sample MTIA 104 yields *E. floralis* and the LAD of *Nannoconus circularis*. The two samples at **MTIA 151** and **MTIA 153** yield a Late Aptian assemblage reminiscent of equivalent deposits investigated at Tiskatine. *M. hoschulzii, C. bosunensis* (common at **MTIA 153**), *Z. vanhintei* and *A. terebrodentarius* ssp. *youngii* are all recorded.

NC8A: A sample from the base of the Oued Tidzi Formation (**MTIA 156**), above the uppermost Aptian – basal Albian unconformity, yielded *P. columnata* and *R. achlyostaurion* together with *C. bosunensis*. *R. parvidentatum* was not recorded in this sample. It appears that *C. bosunensis* ranges into basal Albian deposits. The presence at Id Amran suggests that the lowermost Albian deposits above the basal Albian unconformity are slightly older here than those preserved at Tiskatine where the LAD of *C. bosunensis* is truncated. A more extensive sequence of events including the Lower Albian LO (Last Occurrence) of *C. bosunensis* and *A. terebrodentarius youngii* is recorded at DSDP 370 (see discussion below).

DSDP 370/416

NC6A: At DSDP 370 the exact boundary between the Upper Barremian and Lower Aptian can not be determined based on the calcareous nannofossil data. It is either located at the erosive base of the turbidity current in the upper part of core section 34-1 (872.85–873.26 m) above deposits of NC6A, or located within the core gap above. The base of the turbidite at 873.26 m could correspond to a regional regressive phase recognized at the Barremian - Aptian transition within the Bouzergoun Fm. onshore the EAB.

NC6B: The basal part of core 32-4 (840.42–389.87 m) contains strata of Early Aptian age. These deposits are older than the sedimentary rocks assigned to NC6B from the Id Amran section onshore. Here at DSDP 370 the occurrence of *Z. scutula* indicates the lower part of NC6B.

NC7A: The recorded stratigraphy of NC7A, forming the bulk of the Tiskatine section, is not recorded at DSDP borehole 370.

NC8A: The contact between the lowermost Aptian (NC6B) and Lower Albian sequence (NC8A) lies between 838.57 and 839.87 m. Onshore in the EAB the Aptian/Albian boundary is marked by a regional erosive unconformity and a distinct colour change from blue-grey marls of the Tamzergout Formation to green marls of the Oued Tidzi Formation. This colour change is also observed in the core section 32-4 (838.57–839.87 m, Fig. 6). Therefore, a hiatus and the basal Albian unconformity are tentatively placed at the erosive contact at 839.68 m. It could also fall at the base of the erosive turbidite at 839.87 m. The boundary is thought to correlate to the regional sequence boundary recognized onshore (Luber et al., 2017) and in borehole 370 appears to erode most of the Lower Aptian and all the Upper Aptian strata.

At the adjacent DSDP Borehole 416A the basal Albian unconformity is also recorded within core 6 (CC). Here again, Lower Albian (NC8A) deposits rest directly with a marked hiatus upon lowermost Aptian strata (NC6B).

5.2. Carbon isotope chemostratigraphic correlation

This section provides interpretation of the $\delta^{13}C$ curve in the Tiskatine section and a correlation to the biostratigraphically well-constrained Vocontian basin (Fig. 15).

5.2.1. Interpretation of the $\delta^{13}C$ trend in the Tiskatine section

To discuss our $\delta^{13}C$ dataset it must be assessed that local water cycling processes or diagenesis had no significant influence and the observed $\delta^{13}C$ trends are mainly representative of global change in the carbon cycle. The here-analysed carbonate samples are made of bulk micrite deposited in an open shelf setting and open ocean water masses are expected (Immenhauser et al., 2002). Resetting of $\delta^{13}C_{carb}$ values by late diagenetic processes are unlikely since the abundance of carbonates act as a strong buffer against significant isotopic exchange with C-poor fluids (e.g. Marshall, 1992). The absence of major diagenetic resetting of our $\delta^{13}C_{carb}$ dataset is confirmed by measured values typical for an Aptian oceanic signature, as reported from numerous studies (e.g. Herrle et al., 2004; Bodin et al., 2015). The values of the $\delta^{13}C_{org}$ dataset are similar to McAnena et al. (2013) for DSDP borehole 545.

For the $\delta^{13}C_{carb}$ values, care must be taken for the lowermost (**MTTK 162** – **MTTK 169**) and uppermost (**MTTK 237** – **MTTK 249**) parts of the Tamzergout Formation. Here high amplitude and sharp fluctuation of $\delta^{13}C_{carb}$ values are observed. Since similar trends and fluctuations cannot be observed in the $\delta^{13}C_{org}$ dataset, it can be hypothesized that these high-amplitude and sharp fluctuations of $\delta^{13}C_{carb}$ values are linked to early diagenetic resetting. This is most notably close to the hiatus separating the Tamzergout and Oued Tidzi Fms. The large negative C-isotope excursion at the top of the Tamzergout Fm. resembles a negative excursion associated with subaerial exposure diagenesis due to the adjunction of ^{13}C-depleted carbon derived from soil development (Allan and Matthews, 1982). There is, however, no physical indication for subaerial exposure related to the Lower Albian unconformity at the base of the Oued Tidzi Fm. Oxidation of marine organic matter or local oceanographic conditions related to water masses isolation could thus be a more likely explanation for these two negative excursions.

5.2.2. Correlation to the South Provence and Vocontian Basin

The chemostratigraphic correlation between the EAB and the SE France reference sections established in the South Provence and

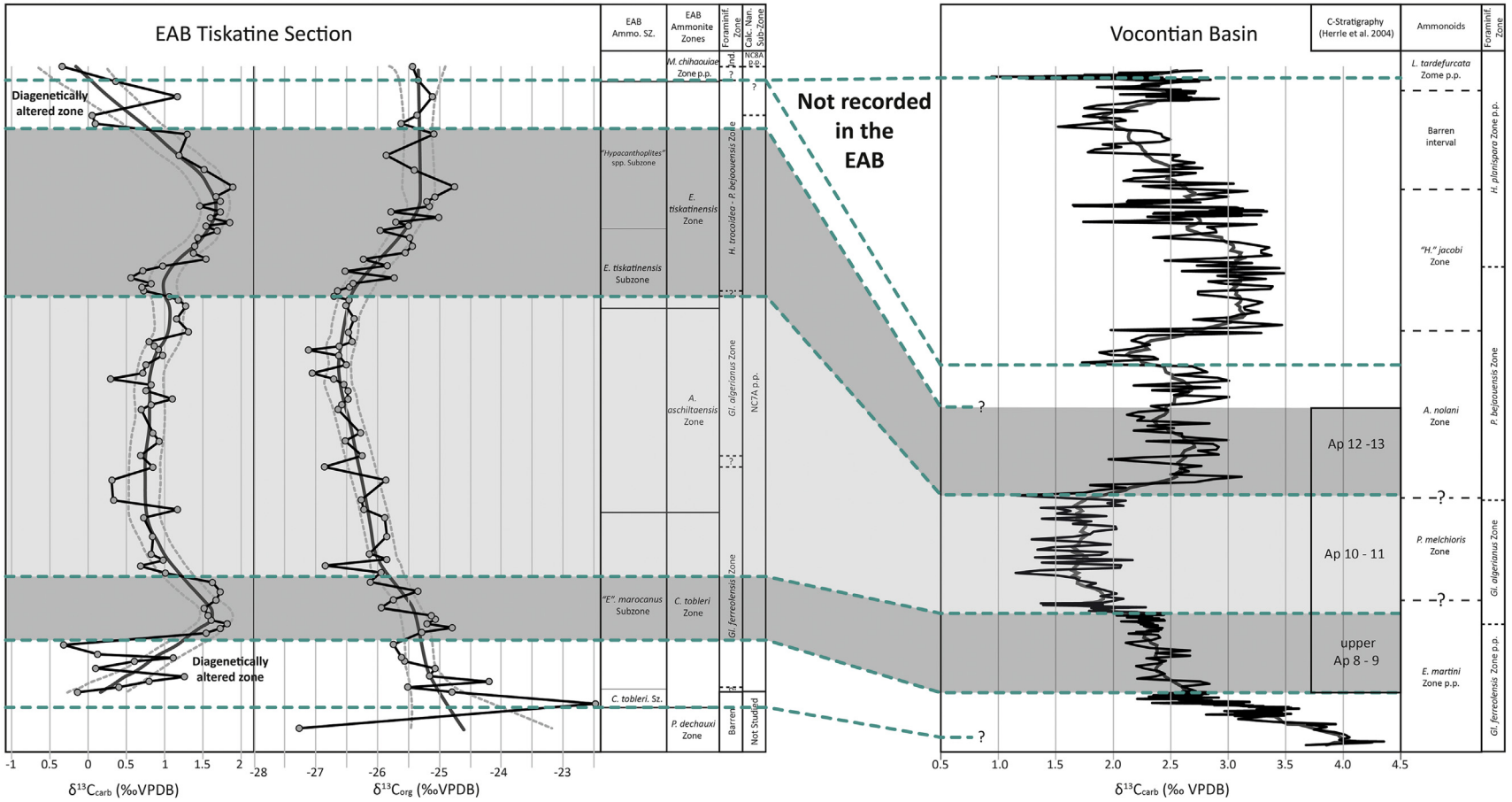

Fig. 15. Comparison of Lower Aptian to Lower Albian $\delta^{13}C_{carb}$ and $\delta^{13}C_{org}$ (‰ VDPB) at Tiskatine, EAB and $\delta^{13}C_{carb}$ (‰ VDPB) in the Vocontian Basin (data from Herrle et al., 2004). Two negative shifts of the succession are highlighted by grey shading bands and diagenetically altered data annotated. Data is references against the local ammonoid zonation scheme in the EAB of Luber et al. (2017), the Standard Mediterranean Ammonite Scale (SMAS) of Reboulet et al. (2011, 2014), standard planktonic foraminiferal zonation of Premoli Silva and Verga (2004) and Lower Cretaceous NC Zones of Roth (1978, 1983) and subzones after Bralower et al. (1993).

Vocontian Basin (Herrle et al., 2004) has to take into account the two basin-wide hiatus recognized in the Tiskatine section, covering 1) the upper *D. forbesi* Zone to lower *E. martini* Zone and 2) the whole *H. jacobi* to lowermost *L. tardefurcata* Zone equivalent of the SMAS. Furthermore, the sedimentary record in the EAB is far more condensed than its counterparts in SE France (Fig. 15).

Considering the hiatus in the EAB and stratigraphic gaps, the overall $\delta^{13}C_{org}$ curve as well as the $\delta^{13}C_{carb}$ curve of the EAB (Fig. 14) matches the established curves of the Vocontian and South Provence basins. The lowermost and uppermost part of the Tiskatine $\delta^{13}C_{carb}$ record cannot be chemostratigraphically correlated to the French reference curve, which corroborates the hypothesis of diagenetic alteration. Eliminating these data allows clear observation of an initial negative $\delta^{13}C$ trend (minimum amplitude of ca. 1‰ for the $\delta^{13}C_{carb}$ record, and 4‰ for the $\delta^{13}C_{org}$ record) that correspond well to the upper part of the decline in $\delta^{13}C$ values spanning the Lower – Upper Aptian transition observed in the Vocontian Basin (in both bulk micrite and belemnite records; Herrle et al., 2004; Bodin et al., 2015), as well as in the South Provence Basin (Kuhnt et al., 2011) and elsewhere (e.g. Menegatti et al., 1998; De Gea et al., 2003; Godet et al., 2014). This decline is a global environmental signal, resulting from a return to pre-OAE 1a positive excursion values (C8 segment of Menegatti et al., 1998; see also Bodin et al., 2015). Given that the C7 segment of Menegatti et al. (1998), i.e. the maximum of the Lower Aptian positive $\delta^{13}C$ (related to the OAE 1a), is not recorded in Tiskatine, it is difficult to assess which exact part of the C8 segment of Menegatti et al. (1998) is represented by the decreasing trend observed in our record. As the here observed decreasing trend falls within the middle to upper *E. martini* Zone equivalent of SMAS, we correlate it to the upper part of the C8 segment (Menegatti et al., 1998).

The following $\delta^{13}C$ plateau in the Tiskatine section (around 0.7‰ for $\delta^{13}C_{carb}$ and around −26.5‰ for $\delta^{13}C_{org}$) can be correlated to the Ap10 and Ap11 segments of Herrle et al. (2004), spanning most of the *G. algerianus*/*H. trocoidea* foraminifera zone. This agrees with our biostratigraphic zonation. Lastly, the $\delta^{13}C$ positive excursion spanning the upper part of the Tiskatine section (excluding the diagenetically altered uppermost part of the $\delta^{13}C_{carb}$ record) and the plateau of $\delta^{13}C_{org}$ in the uppermost part of the section correlates well to the Ap12 and Ap 13 segments of Herrle et al. (2004), supporting the correlation between the *E. tiskatinensis* ammonite Zone in Morocco and the *N. nolani* ammonite Zone in SE France (Luber et al., 2017).

Finally, it should be noted that the $\delta^{13}C_{org}$ value of −27.27‰ for the **MTTK 160** sample at the base of the section is similar to the $\delta^{13}C_{org}$ values observed within the lowermost *A. aschiltaensis* Zone. This is consistent with its earliest Aptian pre-OAE 1a age attribution (*P. dechauxi* Zone, which is the equivalent to the lower part of the *D. forbesi* Zone; Luber et al., 2017). Indeed, in SE France, similar $\delta^{13}C$ values have also been observed for these two intervals (Föllmi et al., 2006; Kuhnt et al., 2011; Bodin et al., 2013, 2015).

The comparison between carbonate and organic matter $\delta^{13}C$ records of the Tiskatine section (Fig. 14) and the Vocontian Basin reference section (Fig. 15) further supports the biostratigraphic scheme established in Morocco. Additionally, the correlation, additionally, confirms that key stratigraphic intervals, the OAE 1a-equivalent and the Aptian/Albian boundary section, are not recorded at Tiskatine.

5.3. The evolution of the EAB during the Aptian

5.3.1. Depositional environment and sequence stratigraphic interpretation

Through palaeontological and field observations, depositional environments and key sequence stratigraphic surfaces are described for the Tiskatine section (Fig. 13). Supporting observations come from the Id Amran and Assaka sections and information from the DSDP boreholes 370/416 is also discussed.

Three 3rd order stratigraphic sequences have been recognised. Interpreted sedimentological logs and field photographs are presented in the supplementary data.

Lower Aptian – Sequence 1

The lower part of the Tiskatine section (**MTTK 157 – 161a**) is dominated by wave-influenced shoreface sedimentation overlain by lower shoreface conditions. The interval is barren in foraminifera and calcareous nannofossil but yields abundant ammonoids. Between **MTTK 159** to **160b** lack in mesopelagic phylloceratids and lytoceratids, and the abundance of the shallow nekton-benthic douvilleiceratid *Prochelonicera*s (Westermann, 1990, 1996) suggest a distal neritic setting (Frau et al., 2017).

A 3rd order **sequence boundary** around the Lower/Upper Aptian boundary is recognized between **MTTK 160b** and **161a**, well constrained by ammonoid biostratigraphy (Luber et al., 2017).

Upper Aptian – Sequence 2

A subsequent initial transgressive surface (**ITS**) and condensation are recognised in **MTTK 161a**. Here the occurrence of phylloceratids and desmoceratids indicates a brief episode of open-marine conditions at the top of the Bouzergoun Fm.; albeit the fauna is still largely dominated by nekton-benthic forms such as *Epicheloniceras*. The rich and diverse mix of epipelagic and mesopelagic assemblages form a typical Type 2 Horizon of Faunal Uniformity (HUF) and is interpreted to be the result of sea level rise and flooding events (Bulot, 1993).

In **MTTK 162** a rapid increase in water depth and the establishment of shelfal conditions is indicated by first occurrence planktonic nannoflora and an increase in foraminifera and calcareous nannofossil recovery. A lithological disconformity from sandstones to marls and increased carbonate content is also recognised between **MTTK 162 and 163.**

The establishment of shelfal conditions at Id Amran predates (*P. dechauxi* Zone) the establishment at Tiskatine (*C. tobleri* Zone), while at Assaka this time interval is marked as erosive surfaces.

The increase in base-level recognized in **MTTK 162** can be observed regionally and is interpreted as a 3rd order **transgressive systems tract** (**TST**) starting with **MTTK 161a**.

Between **MTTK 164 – MTTK 232** the proportion of planktonic foraminifera seldom falls below 50%, indicating water depths of 50–200 m (Murray, 1991) suggesting middle to outer shelf conditions. High relative abundance (65%–81%) of planktonic foraminifera (notably *Hedbergella* spp.), a prominent increase in abundance and diversity of calcareous nannofossil from **MTTK 162** through to **MTTK 165b,** and higher carbonate content suggest good open-marine conditions. Therefore, **MTTK 164/165** ("*E.*" *marocanus* Subzone) is interpreted as a **Lower Upper Aptian maximum flooding surface (MFS)**. Regional flooding within the *C. tobleri* Zone is followed by relative continuous deposition in the Tiskatine and Id Amran sections and is also recorded at Assaka (**MTAS 121**).

The interval from **MTTK 166–191** is interpreted as multiple parasequences in a third order **high stand systems tract (HST)**. Sample **MTTK 183b** contains common reworked *Epistomina* derived from shallow shelf environments. The abundance of ammonites decreases significantly and fauna is dominated by the endemic "*E.*" *marocanus*. The same is true at Id Amran between **MTIA 109** to **130.**

Between **MTTK 184** to **194**, and even up to **MTTK 203** the ammonite fauna is characterised by the abundance of the cosmopolitan *A. aschiltaensis* and *P.* gr. *ramososeptatum* indicating

restored open-marine connections between the EAB and the Mediterranean-Caucasian Tethys. This is also recognised at Id Amran (**MTIA 131** to **142**) and elements are further recorded in Assaka (**MTAS 123**).

MTTK 192 stands out in the field characterised by an erosive base, interpreted as a 3rd order **sequence boundary**. **MTTK 192** has higher siliciclastic content and is barren of foraminifera, but yields large ammonoids (*Pseudoaustraliceras*).

The Lower Aptian succession is expanded at Id Amran compared to Tiskatine. This changes above the regional flooding in the *C. tobleri* Zone and the Upper Aptian succession is compressed in Id Amran compared to Tiskatine and the Id Amran section records a higher siliciclastic input.

Upper Aptian – Sequence 3

The top of **MTTK 194** is interpreted as the **ITS.** A rich and diverse ammonite assemblage between **MTTK 206 – MTTK 213** and increased recovery of foraminifera and calcareous nannofossils between **MTTK 211 – MTTK 215** suggest the presence of an **Upper Aptian MFS** between **MTTK 206 – MTTK 215** (*E. tiskatinensis* Subzone) with Horizons of Faunal Uniformity. This brackets a 3rd order transgressive systems tract (**TST**) between top **MTTK 194** and **MTTK 215**, which is also recognised at **Id Amran** (**MTIA 149 – 150 top**). At Assaka elements of the *E. tiskatinensis* Subzone are also recorded in poly-phased horizons and polyzonal lenses (**MTAS 123**) infilling erosional surfaces.

Overall the upper part of the Tamzergout Fm. at Tiskatine, particularly **MTTK 206** to **231**, is marked by the high abundance and diversity of small-sized epipelagic forms (*Elsaisabellia*, *Protacanthoplites* and "*Hypacanthoplites*") combined with spot occurrences of mesopelagic desmoceratids, indicating the restoration of fully open-marine condition.

The interval **MTTK 216 to MTTK 247** is overall still rich in foraminifera, but the interval from **MTTK 232** to **247** is barren in ammonoids and a continuous decline of planktonic foraminifera (50% to <30%) is noted from **MTTK 233** upward. Further, reworking of shelfal *Epistomina* is particularly evident in **MTTK 223 – MTTK 237**. Calcareous nannofossils are still abundant in this interval, with **MTTK 239** yielding the richest nannoflora of the whole section. Therefore, **MTTK 216 – MTTK 247** is interpreted as a **HST.** This interval is absent at Id Amran.

Clastic progradation is heralded by a marked reduction in diversity and abundance of calcareous nannofossils in bed **MTTK 247. MTTK 247** further shows a noteworthy increase in abundance of reworked *Epistomina* (the highest numbers recorded in any sample). Obviously transported specimens may be indicative of episodes of shelf erosion and redeposition. It is uncertain if these are the results of autocyclic processes affecting the shelf (e.g. severe storms) or of allocyclic processes such as lowering of relative sea-level. Increase in abundance of *Epistomina* and diversity decrease of calcareous nannofossils may indicate of the onset of a shallowing event which ultimately led to the development of a **sequence boundary** at the base of **MTTK 248** identified at Tiskatine. This sequence boundary is more notably expressed at Id Amran (base **MTIA 154**) and DSDP boreholes 370 and 416. At DSDP 370 all the Lower and Upper Aptian succession exposed at Tiskatine is eroded and only older Lower Aptian strata is preserved (NC6B). Boreholes 370/416 are located to the north of the Essaouira-Agadir Basin in the offshore part of the Doukalla Basin and, therefore, not necessarily directly tied to the evolution of the EAB. Nonetheless, the prominently and apparently regionally-developed uppermost Aptian to Lower Albian sequence boundary is noteworthy. This boundary possibly combines a 3rd and 2nd order sequence boundary. It is well constrained by ammonoids, foraminifera and calcareous nannofossils to occur between the "*Hypacanthoplites* spp." Subzone and the *M. chihaouiae* Zone and is, therefore, suspected as being close to the Aptian/Albian boundary. Relating this sequence boundary to published eustatic sea-level curves is challenging, but it is here tentatively linked to KAp 7 *sensu* Haq (2014).

A sample from bed **MTTK 249** exhibits a dramatic change in palaeoenvironmental conditions compared to the underlying Aptian deposits. Neritic dominated holococcoliths and nannoconids are rarely recorded whilst a cold-water incursion of *R. parvidentatum* is recorded. A regional palaeo-oceanographic change reflected in the nannofossil assemblage appears to have occurred at the Aptian/Albian boundary.

5.3.2. Palaeogeographic interpretation

Early Aptian

A transect from Id Amran to Assaka (Fig. 16) shows a thinning succession, interpreted to be controlled by reducing accommodation toward the crest of a submerged fault block. During the Early Aptian, the following incremental tectonic movement phases can be dated by ammonoid biostratigraphic data along this transect:

- *P. dechauxi* – lower *D. forbesi* zones: Constrained by erosion of *P. dechauxi* – *C. tobleri* zones time-equivalent deposits in the distal Assaka section (erosional surface base **MTAS 121**). These zones are present in Tiskatine (**MTTK 159–160b**) and Id Amran (**MTIA 86 – MTIA 98**). In Id Amran preservation of the *D. forbesi* Zone time-equivalent deposits (**MTIA 98**) further constraints the timing of first movement phase.
- Lower *D. forbesi* – *D. furcata* zones: Constrained by absence of the upper *D. forbesi* plus the entire *D. deshayesi* zones (=OAE 1a-related time culmination) in Id Amran. *D. forbesi* and *D. furcata* zone age deposits are not recorded in Tiskatine and Assaka and form part of a composite surface including multiple unconformities (hiatus **MTTK 160b – MTTK 161a** and again erosional surface base **MTAS 121**).
- *D. furcata* – *C. tobleri* zones: Unconformity constrained by absence of the upper *D. furcata* Zone in Id Amran

Early Aptian tectonic movement phases (1) to (3) are expressed in the sedimentary record as disconformities, generally as surfaces of non-deposition. In the Assaka section, they are combined into the basal erosional surface of **MTAS 121**.

Late Aptian

While the Early Aptian was marked by increased accommodation and early establishment of shelfal conditions in the Id Amran area, this changed in the Late Aptian. The compressed Upper Aptian succession compared to Tiskatine is interpreted as a gradual infill of accommodation and onlap towards the crest of the submerged fault block to the west. The absence of the "*Hypacanthoplites*" spp. Subzone at Id Amran is linked to stronger erosion than in Tiskatine at the uppermost Aptian to basal Albian sequence boundary.

Towards the crest of the fault block in Assaka the Upper Aptian is recorded as a set of horizons marked by poly-phased erosion and sedimentation (**MTAS 122** and **123**). Preserved ammonoid specimens mainly coincide with Late Aptian–earliest Albian flooding events in the basin suggesting continuous reworking on the crest of a submerged fault block. It is noteworthy that among the ammonoid assemblage in lenses of **MTAS 123** open-marine fauna (*Hypophylloceras*, *Eotetragonites* and *Ephamulina*) are well-represented. This suggests the crest of the submerged fault block

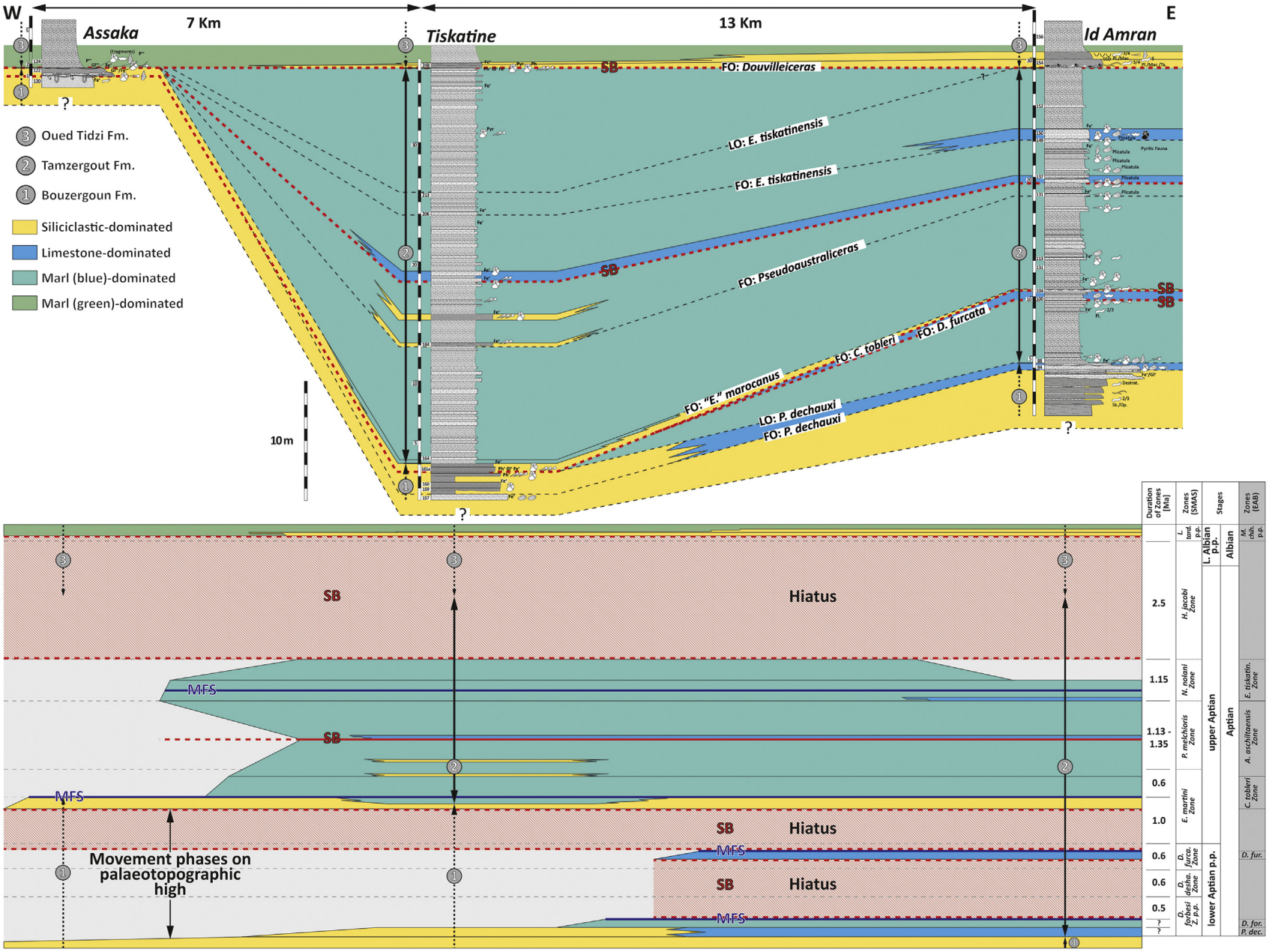

Fig. 16. Sequence stratigraphic correlation of the Id Amran, Tiskatine and Assaka section based on ammonoid biostratigraphy with associated Wheeler Diagram. Data is referenced to the local ammonoid zonation scheme in the EAB of Luber et al. (2017), the Standard Mediterranean Ammonite Scale (SMAS) of Reboulet et al. (2011, 2014). Duration of ammonoid zones are derived from Dauphin, 2002.

was located on the outer shelf, below storm wave base, open to the ocean in the west and that lenses (**MTAS 123**) formed through winnowing by wave-action and mixing of faunal elements. The N-S orientated crest was located in proximity of the modern coastline.

6. Conclusions

This paper presents combined high-resolution litho-, bio-, chemo- and sequence stratigraphic data analysis for the Aptian of the NW African Atlantic margin. A reference section is proposed at Tiskatine, offering the most complete outcropping section encountered in the EAB. The results provide new information on ranges of foraminifera and calcareous nannofossils, which importantly have been correlated with the local ammonoid zonation scheme defined for the EAB by Luber et al. (2017). Their wider correlation against type localities and species (e.g. SMAS) is discussed. This study also extends the growing global body of $\delta^{13}C$ data against a high-resolution, biostratigraphically constrained section.

Based on the distribution of foraminifera in the Tiskatine section, three widely used Upper Aptian zones have been recognized: *G. ferreolensis* Zone, *G. algerianus* Zone, and *H. trocoidea – P. bejaouensis* zones. In addition, two standard calcareous nannofossil zones are recognised at Tiskatine: NC7A and NC8A. The calibration of these zones against the SMAS and hence standard chronostratigraphy, implies crucial revisions to previously reported ranges.

The $\delta^{13}C_{org}$ curve, as well as the $\delta^{13}C_{carb}$ curve, support the biostratigraphic analysis at Tiskatine and can be correlated with the established curves of the Vocontian and South Provence Basin in SE France. The $\delta^{13}C$ analysis highlights the absence of the OAE 1a equivalent time interval and the uppermost Aptian interval, as indicated by biostratigraphic data.

Foraminifera, calcareous nannofossil, and carbon isotope data support the presence of a regional hiatus at the Aptian/Albian boundary in the EAB. Revised age dating using calcareous nannofossils at DSDP boreholes 370 and 416 further indicates the presence of this hiatus associated with a regional unconformity offshore.

Based on the integration of biostratigraphic data and sedimentological observations, local tectonics can be discerned during the Aptian along the Atlantic Margin.

The robust chronostratigraphic framework presented is a contribution towards regional and super-regional correlations that will aid future palaeo(bio)geographic interpretations.

Acknowledgements

This study forms part of the lead authors PhD at the University of Manchester with the North Africa Research Group (NARG). The authors would like to thank the sponsoring companies of NARG and L'Office National des Hydrocarbures et des Mines (ONHYM) for their continued logistical and scientific support. The constructive comments of the editor-in-chief, two anonymous reviewers, and Dr. Christian Linnert (Ruhr-Universität, Bochum) are highly appreciated and improved the manuscript greatly. We thank David Gelsthorpe and the team of the Manchester Museum for curation of all the figured material of this publication. Dr Colin Harris (Hydrocarbons International) is thanked for his role in assisting with the foraminiferal analysis. The Natural History Museum is thanked for allowing access to their SEM facility. Prof. Paul Bown at University College London is thanked for access to nannofossil photographic equipment. Prof. Jens O. Herrle (Goethe-Universität, Frankfurt) and Prof. Wolfgang Kuhnt (Christian-Albrechts-Universität, Kiel) are thanked for providing us with their original $\delta^{13}C$ data for Vocontian and South Provence basins. Dr. Gérard Friès (Areva, Astana, Kazakhstan) is thanked for his invaluable support during the revision of the French standard successions. We would further like to acknowledge all field assistants and their invaluable help and input.

References

Aguado, R., Castro, J.M., de Gea, G.A., 1999. Aptian bio-events – an integrated biostratigraphic analysis of the Almadich Formation, Inner Prebetic Domain, SE Spain. Cretaceous Research 20, 663–683.

Allan, J.R., Matthews, R.K., 1982. Isotope signatures associated with early meteoric diagenesis. Sedimentology 29, 797–817.

Ambroggi, R., 1963. Etude géologique du versant méridional du Haut-Atlas occidental et de la plaine du Souss. Notes et Mémoires du Service Géologique du Maroc 157, 1–322.

Ando, A., Huber, B.T., Premoli Silva, I., 2013. *Paraticinella rohri* (Bolli, 1959) as the valid name for the latest Aptian zonal marker species of planktonic foraminifera traditionally called *bejaouaensis* or *eubejaouaensis*. Cretaceous Research 45, 275–287.

Armstrong, H.A., Brasier, M.D., 2005. Microfossils. Blackwell Publishing Ltd (Wiley-Blackwell), Oxford, 296pp.

Bartenstein, H., Bettenstaedt, F., 1962. Marine Unterkreide (Boreal and Tethys). In: Simon, W., Bartenstein, H. (Eds.), Leitfossilen der Mikropaläontologie. Gebrüder Borntraeger, Berlin, pp. 225–298.

Baudin, F., Moullade, M., Tronchetti, G., 2008. Characterisation of the organic matter of upper Bedoulian and lower Gargasian strata in the historical stratotypes (Apt and Cassis-la-Bédoule areas, SE France). Carnets de Géologie/Notebooks on Geology 01, 1–9.

Behrens, M., Krumsiek, K., Meyer, D.E., Schäfer, A., Siehl, A., Stets, J., Thein, J., Wurster, P., 1978. Sedimentationsabläufe im Atlas-Golf (Kreide Küstenbecken Marokko). Geologische Rundschau 67, 424–453.

Bellier, J.P., Moullade, M., 2002. Lower Cretaceous planktonic foraminiferal biostratigraphy of the western North Atlantic (ODP Leg 171B), and taxonomic clarification of key index species. Revue de Micropaleontologie 45, 9–26.

Bergen, J.A., 2000. Calcareous Nannofossils from the Lower Aptian Historical Stratotype at Cassis-La Bédoule (SE France). In: Moullade, M., Tronchetti, G., Masse, J.-P. (Eds.), Le stratotype historique de l'Aptien inférieur (Bédoulien) dans la région de Cassis-La Bédoule (S.E. France), Géologie méditerranéenne 25/3-4 (1998), pp. 227–255.

Bodin, S., Godet, A., Westermann, S., Föllmi, K.B., 2013. Secular change in northwestern Tethyan water-mass oxygenation during the Late Hauterivian-Early Aptian. Earth and Planetary Science Letters 374, 121–131.

Bodin, S., Meissner, P., Janssen, N.M.M., Steuber, T., Mutterlose, J., 2015. Large igneous provinces and organic carbon burial: Controls on global temperature and continental weathering during the Early Cretaceous. Global and Planetary Change 133, 238–253.

Bodin, S., Hönig, M.R., Krencker, F.-N., Danisch, J., Kabiri, L., 2017. Neritic carbonate crisis during the Early Bajocian: Divergent responses to a global environmental perturbation. Palaeogeography, Palaeoclimatology, Palaeoecology 468, 184–199.

BouDagher-Fadel, M.K., Banner, F.T., Whittaker, J.E., with a contribution from M. D. Simmons, 1997. The Early Evolutionary History of Planktonic Foraminifera. British Micropalaeontological Society Public Series. Chapman and Hall, London, 269 pp.

Bown, P.R., Young, J.R., 1998. Techniques. In: Bown (Ed.), Calcareous Nannofossil Biostratigraphy, pp. 16–28.

Bown, P., Rutledge, D., Crux, J.A., Gallagher, L.T., 1998. Lower Cretaceous. In: Bown, P. (Ed.), Calcareous Nannofossil Biostratigraphy. Chapman and Hall; Kluwer Academic, pp. 86–131.

Bralower, T.J., Sliter, W.V., Arthur, M.A., Leckie, M.R., Allard, D., Schlanger, S.O., 1993. Dysoxic/Anoxic Episodes in the Aptian-Albian (Early Cretaceous). In: Pringle, M.S., Sager, W.S., Sliter, W.V., Stein, S. (Eds.), The Mesozoic Pacific. Geology, Tectonics and Volcanism. Geophysical Monograph Series 77, pp. 5–37.

Bulot, L.G., 1993. Stratigraphical implications of the relationship between ammonites and facies; examples from the Lower Cretaceous (Valanginian–Hauterivian) of the Western Tethys. In: House, M.R. (Ed.), The Ammonoidea: Environment, Ecology and Evolutionary Change, The Systematics Association Special Volume 47, pp. 243–265.

Bulot, L.G., 2010. Appendix. Systematic palaeontology of Aptian and Albian ammonites from southwest Iran. In: Vincent, B., van Buchem, F.S.P., Bulot, L.G., Immenhauser, A., Caron, M., Baghbani, D., Huc, A.Y. (Eds.), Carbon–Isotope Stratigraphy, Biostratigraphy and Organic Matter Distribution in the Aptian-Lower Albian Successions of Southwest Iran (Dariyan and Kazhdumi Formations). GeoArabia Special Publication 4/1, pp. 167–195.

Bulot, L.G., Latil, J.-L., Hairabian, A., Fournillon, A., 2014. New insight on the genus *Nolaniceras* Casey, 1961 (Ammonoidea, Cretaceous) and its consequences on the biostratigraphy of the Aptian Stage. Proceedings of the Geologists' Association 125, 227–232.

Butt, A., 1982. Micropaleontological bathymetry of the Cretaceous of western Morocco. Palaeogeography, Palaeoclimatology, Palaeoecology 37, 235–275.

Caron, M., 1985. Cretaceous planktonic foraminifera. In: Bolli, H.M., Saunders, J.B., Perch-Nielsen, K. (Eds.), Plankton Stratigraphy. Cambridge University Press, pp. 17–86.

Damotte, R., Magniez-Jannin, F., 1973. Ostracodes et foraminifères de l'Aptien inférieur du Sondage du Bois du Perchois (Aube). Bulletin d'Information des Geologues du Bassin de Paris 36, 3–47.
Dauphin, L., 2002. Litho-, bio-, et chronostratigraphie comparées dans le Bassin vocontien à l'Aptien. Unpublished PhD Thesis. Université de Lille 1, 451 pp.
De Gea, G.A., Castro, J.M., Aguado, R., Ruiz-Ortiz, P.A., Company, M., 2003. Lower Aptian carbon isotope stratigraphy from a distal carbonate shelf setting: the Cau section, Prebetic zone, SE Spain. Palaeogeography, Palaeoclimatology, Palaeoecology 200, 207–219.
Duffaud, F., Brun, L., Planchut, B., 1966. Le bassin du Sud-Ouest marocain. In: Reyre, D. (Ed.), Bassins sédimentaires du Littoral africain. Symposium de l'Association des Services géologiques africains (New Dehli, 1964). 1ère partie, Littoral Atlantique, 5–12. Firmin Didot Publications, Paris.
Dutour, Y., 2005. Biostratigraphie, évolution et renouvellements des ammonites de l'Aptien supérieur (Gargasien) du bassin vocontien (Sud–Est de la France). Unpublished PhD Thesis. Lyon 1, 302 pp.
Ettachfini, M., Company, M., Jaques, R., Taj-Eddine, K., Tavera, J.M., 1998. Le Valanginien du bassin de Safi (Maroc atlantique) et sa faune d'ammonites. Implications paléobiogéographiques. Comptes Rendus de l'Académie des Sciences de Paris, Sciences de la Terre et des Planètes 327, 319–325.
Föllmi, K.B., Godet, A., Bodin, S., Linder, P., 2006. Interactions between environmental change and shallow-water carbonate build-up along the northern Tethyan margin and their impact on the Early Cretaceous carbon-isotope record. Paleoceanography 21 (PA4211), 1–16.
Frau, C., Delanoy, G., Hourquieg, E., 2015. Le genre *Macroscaphites* Meek, 1876 (Ammonoidea) dans l'Aptien inférieur de Cassis-La Bédoule (Bouches-du-Rhône, France). Proposition d'un nouveau schéma zonal pour la série stratotypique. Revue de Paléobiologie 34, 45–57.
Frau, C., Delanoy, G., Masse, J.-P., Lanteaume, C., Tendil, A.J.B., 2016. New Heteroceratidae (Ammonoidea) from the Late Barremian deepening succession of Marseille (Bouches–du–Rhône, France). Acta Geologica Polonica 66/2, 179–199.
Frau, C., Pictet, A., Spangenberg, J., Masse, J.-P., Tendil, A.J.B., Lanteaume, C., 2017. New insights on the age of the post-Urgonian marly cover of the Apt region (Vaucluse, SE France) and its implications on the demise of the North Provence carbonate platform. Sedimentary Geology 359, 44–61.
Frau, C., Bulot, L.G., Delanoy, G., Moreno-Bedmar, J.A., Masse, J.-P., Tendil, A.J.-B., Lanteaume, C., 2018. The candidate Aptian GSSP at Gorgo a Cerbara (Central Italy): an alternative interpretation of the bio-, litho- and chemostratigraphic markers. Newsletter on Stratigraphy 51, 311–326.
Godet, A., Hfaiedh, R., Arnaud-Vanneau, A., Zghal, I., Arnaud, H., Ouali, J., 2014. Aptian palaeoclimates and identification of an OAE1a equivalent in shallow marine environments of the southern Tethyan margin: Evidence from Southern Tunisia (Bir Oum Ali section, Northern Chott Chain). Cretaceous Research 48, 110–129.
Haq, B., 2014. Cretaceous eustasy revisited. Global and Planetary Change 113, 44–58.
Herrle, J.O., Mutterlose, J., 2003. Calcareous nannofossils from the Aptian–Lower Albian of southeast France: palaeoecological and biostratigraphic implications. Cretaceous Research 24, 1–22.
Herrle, J.O., Kössler, P., Friedrich, O., Erlenkeuser, H., Hemleben, C., 2004. High-resolution carbon isotope records of the Aptian to Lower Albian from SE France and the Mazagan Plateau (DSDP Site 545): a stratigraphic tool for paleoceanographic and paleobiologic reconstruction. Earth and Planetary Science Letters 218, 149–161.
Immenhauser, A., Kenter, J.A.M., Ganssen, G., Bahamonde, J.R., Van Vliet, A., Saher, M.H., 2002. Origin and Significance of Isotope Shifts in Pennsylvanian Carbonates (Asturias, NW Spain). Journal of Sedimentary Research 72, 82–94.
Jeremiah, J., 1996. A proposed Albian to lower Cenomanian nannofossil biozonation for England and the North Sea basin. Journal of Micropalaeontology 15, 97–129.
Jeremiah, J., 2000. Lower Cretaceous turbidites of the Moray Firth: sequence stratigraphical framework and reservoir distribution. Petroleum Geoscience 6, 309–328. Supplementary Publication No. SUP 18155, 1-19.
Jeremiah, J., 2001. A Lower Cretaceous nannofossil zonation for the North Sea Basin. Journal of Micropalaeontology 20, 45–80.
Jeremiah, J.M., Duxbury, S., Rawson, P., 2010. Lower Cretaceous of the southern North Sea Basins: reservoir distribution within a sequence stratigraphic framework. Netherlands Journal of Geosciences/Geologie en Mijnbouw 89, 203–237.
Kennedy, W.J., Gale, A.S., Bown, P.R., Caron, M., Davey, R.J., Gröcke, D., Wray, D.S., 2000. Integrated stratigraphy across the Aptian-Albian boundary in the Marnes Bleues, at the Col Pré-Guittard, Arnayon (Drôme), and at Tartonne (Alpes-de-Haute-Provence), France: a candidate Global Boundary Stratotype Section and Boundary Point for the base of the Albian Stage. Cretaceous Research 21, 591–720.
Kennedy, W.J., Gale, A.S., Huber, B.T., Petrizzo, M.R., Bown, P., Barchetta, A., Jenkyns, H.C., 2014. Integrated stratigraphy across the Aptian/Albian boundary at Col de Pré-Guittard (southeast France): A candidate Global Boundary Stratotype Section. Cretaceous Research 51, 248–259.
Kilian, W., Gentil, L., 1906. Découverte de deux horizons crétacés remarquables au Maroc. Comptes rendus sommaire de l'Académie des Sciences de Paris 142, 603–605.
Kuhnt, W., Moullade, M., 2007. The Gargasian (Middle Aptian) of La Marcouline section at Cassis-La Bédoule (SE France): Stable isotope record and orbital cyclicity. Carnets de Géologie. Article 2007/02, 9 p.
Kuhnt, W., Holbourn, A., Moullade, M., 2011. Transient global cooling at the onset of Early Aptian oceanic anoxic event (OAE) 1a. Geology 39, 323–326.
Latil, J.-L., 2011. Early Albian ammonites from Central Tunisia and adjacent areas of Algeria. Revue de Paléobiologie 30/1, 321–429.
Laville, E., Pique, A., Amrhar, M., Charroud, M., 2004. A restatement of the Mesosoic Atlasic Rifting (Morocco). Journal of African Earth Sciences 38, 145–153.
Lehmann, J., Friedrich, O., von Bargen, D., Hemker, T., 2012. Early Aptian bay deposits at the southern margin of the lower Saxony Basin: Integrated stratigraphy, palaeoenvironment and OAE 1a. Acta Geologica Polonica 62 (1), 35–62.
Lehmann, J., von Bargen, D., Engelke, J., Claßen, J., 2016. Morphological variability in response to palaeoenvironmental change – a case study on Cretaceous ammonites. Lethaia 49, 73–86.
Luber, T.L., Bulot, L.G., Redfern, J., Frau, C., Arantegui, A., Masrour, M., 2017. A revised ammonoid biostratigraphy for the Aptian of NW Africa: Essaouira-Agadir Basin, Morocco. Cretaceous Research 79, 12–34.
Marshall, J.D., 1992. Climatic and oceanographic isotopic signals from the carbonate rock record and their preservation. Geological Magazine 129 (2), 143–160.
McAnena, A., Flögel, S., Hofmann, P., Herrle, J.O., Griesand, A., Pross, J., Talbot, H.M., Rethemeyer, J., Wallmann, K., Wagner, T., 2013. Atlantic cooling associated with a marine biotic crisis during the mid-Cretaceous period. Nature Geoscience 6, 558–561.
Menegatti, A.P., Weissert, H., Brown, R.S., Tyson, R.V., Farrimond, P., Strasser, A., Caron, M., 1998. High-resolution $\delta^{13}C$ stratigraphy through the Early Aptian "Livello Selli" of the Alpine Tethys. Paleoceanography 13, 530–545.
Meyer, D., 1978. Microfacies and microfabrics of Early Middle Cretaceous sediments selected from site 370, DSDP Leg 41 (deep basin off Morocco). In: Gardner, J., Herring, J. (Eds.), Initial Reports of the Deep Sea Drilling Project 41, pp. 961–981.
Moullade, M., 1966. Étude stratigraphique et micropaléontologique du crétacé inférieur de la "fosse vocontienne". Documents des Laboratoires de Géologie de la Faculté des Sciences de Lyon 15, 1–369.
Moullade, M., Tronchetti, G., Busnardo, R., Masse, J.-P., 2000. Description lithologique des coupes types du stratotype historique de l'Aptien inférieur dans la région de Cassis-La Bédoule (SE France). In: Moullade, M., Tronchetti, G., Masse, J.-P. (Eds.), Le stratotype historique de l'Aptien inférieur (Bédoulien) dans la région de Cassis-La Bédoule (S.E. France), Géologie méditerranéenne 25/3-4 (1998), pp. 15–29.
Moullade, M., Bellier, J.P., Tronchetti, G., 2002. Hierarchy of criteria, evolutionary processes and taxonomic simplification in the classification of Lower Cretaceous planktonic foraminifera. Cretaceous Research 23, 111–148.
Moullade, M., Tronchetti, G., Bellier, J.P., 2005. The Gargasian (Middle Aptian) strata from Cassis-La Bédoule (Lower Aptian historical stratotype, SE France): planktonic and benthic foraminiferal assemblages and biostratigraphy. Carnets de Géologie. Article CG2005_A02.
Murray, J.W., 1991. Ecology and Palaeoecology of Benthic Foraminifera. Wiley, 397 pp.
Nouidar, M., Chellai, H., 2001. Facies and sequence stratigraphy of a Late Barremian wave-dominated deltaic deposit, Agadir Basin, Morocco. Sedimentary Geology 150, 375–384.
Ogg, J.G., Hinnov, L.A., 2012. Cretaceous. In: Gradstein, F.M., Ogg, J.G., Schmitz, M., Ogg, G. (Eds.), The Geologic Time Scale 2012. Elsevier, pp. 793–853.
Owen, H.G., 1996. Boreal and Tethyan Late Aptian to Late Albian ammonite zonation and palaeobiogeography. Mitteilungen aus dem Geologisch-Palaontologischen Institut der Universitat Hamburg 77, 461–481.
Peybernes, C., Giraud, F., Jaillard, E., Robert, E., Masrour, M., Aoutem, M., Içame, N., 2013. Stratigraphic framework and calcareous nannofossil productivity of the Essaouira-Agadir Basin (Morocco) during the Aptian-Early Albian: Comparison with the north-Tethyan margin. Cretaceous Research 39, 149–169.
Phelps, M.R., Kerans, C., Da-Gama, R.O.B.P., Jeremiah, J., Hull, D., Robert, G., Loucks, R.G., 2015. Response and recovery of the Comanche carbonate platform surrounding multiple Cretaceous oceanic anoxic events, northern Gulf of Mexico. Cretaceous Research 54, 117–144 (Supplementary Data).
Premoli Silva, I., Verga, D., 2004. Practical Manual of Cretaceous Planktonic Foraminifera. In: Verga, D., Rettori, R. (Eds.), International School on Planktonic Foraminifera, Universities of Perugia and Milano. Tipografia Pontefelcino, Perugia.
Reboulet, S., Rawson, P.F., Moreno-Bedmar, J.A., reporters), Aguirre-Urreta, M.B., Barragán, R., Bogomolov, Y., Company, M., González-Arreola, C., Idakieva Stoyanova, V., Lukeneder, A., Matrion, B., Mitta, V., Randrianaly, H., Vašíček, Z., Baraboshkin, E.J., Bert, D., Bersac, S., Bogdanova, T.N., Bulot, L.G., Latil, J.-L., Mikhailova, I.A., Ropolo, P., Szives, O., 2011. Report on the 4th International Meeting of the IUGS Lower Cretaceous Ammonite Working Group, the "Kilian Group" (Dijon, France, 30th August 2010). Cretaceous Research 32, 786–793.
Reboulet, S., Szives, O., Aguirre-Urreta, B., Barragán, R., Company, M., Idakieva, V., Ivanov, M., Kakabadze, M.V., Moreno-Bedmar, J.A., Sandoval, J., Baraboshkin, E.J., Çağlar, M.K., Főzy, I., González-Arreola, C., Kenjo, S., Lukeneder, A., Raisossadat, S.N., Rawson, P.F., Tavera, J.M., 2014. Report on the 5th International Meeting of the IUGS Lower Cretaceous Ammonite Working Group, the Kilian Group (Ankara, Turkey, 31st August 2013). Cretaceous Research 50, 126–137.
Rey, J., Canérot, B., Peybernès, B., Taj-Eddine, K., Rahhali, I., Thieuloy, J.-P., 1986. Le Crétacé inférieur de la région d'Essaouira: données biostratigraphiques et évolutions sédimentaires. Revue de la Faculté des Sciences de Marrakech, Numéro spécial 2, 413–411.

Rey, J., Canérot, J., Peybernès, B., Taj-Eddine, K., Thieuloy, J.-P., 1988. Lithostratigraphy, biostratigraphy and sedimentary dynamics of the Lower Cretaceous deposits on the northern side of the western High Atlas (Morocco). Cretaceous Research 9, 141–158.
Robaszynski, F., Caron, M., 1995. Foraminiferes planctoniques du Crétacé: commentaire de la zonation Europe-Méditerranée. Bulletin de la Societe Geologique de France 166, 681–692.
Roch, E., 1930. Etudes géologiques dans la région méridionale du Maroc Occidental. Notes et Mémoires du Service des Mines et de la Cartes Géologiques Maroc 9, 1–542.
Roth, P.H., 1978. Cretaceous nannoplankton biostratigraphy and oceanography of the northwestern Atlantic Ocean. In: Initial Reports of the Deep-Sea Drilling Project 44, pp. 731–759.
Roth, P.H., 1983. Jurassic and Lower Cretaceous calcareous nannoplankton in the western North Atlantic (Site534): biostratigraphy, preservation and some observations on biogeography and palaeoceanography. In: Winterer, E.L., Ewing, J.I. (Eds.), Initial Reports of the Deep Sea Drilling Projects, 76, pp. 587–621.
Sigal, J., 1977. Essai de zonation du Crétacé du Méditerrannéen a l''aide des foraminiféres planctoniques. Geologie Mediterraneenne 4, 99–108.
Street, C., Bown, P.R., 2000. Palaeobiogeography of Early Cretaceous (Berriasian-Barremian) calcareous nannoplankton. Marine Micropaleontology 39, 265–291.
Tari, G., Jabour, H., 2013. Salt tectonics along the Atlantic margin of Morocco. Geological Society, London, Special Publications 369, 337–353.
Tremolada, F., Erba, E., 2002. Morphometric analysis of the Aptian *Rucinolithus terebrodentarius* and *Assipetra infracretacea* nannoliths: implications for taxonomy, biostratigraphy and paleoceanography. Marine Micropaleontology 44, 77–92.
Verga, D., Premoli Silva, I., 2003a. Early Cretaceous planktonic foraminifera from the Tethys: the large, many–chambered representatives of the genus *Globigerinelloides*. Cretaceous Research 24, 661–690.
Verga, D., Premoli Silva, I., 2003b. Early Cretaceous planktonic foraminifera from the Tethys: small few–chambered representatives of the genus *Globigerinelloides*. Cretaceous Research 24, 305–334.
Westermann, G.E.G., 1990. New developments in ecology of Jurassic–Cretaceous Ammonoids. In: Pallini, G., Cecca, F., Cresta, S., Santantonio, M. (Eds.), Fossili, Evoluzione, Ambiente, Atti del Secondo Convegno Internazionale, Pergola, 1987. Comite Centenerio Raffaele Piccinini, pp. 459–478.
Westermann, G.E.G., 1996. Ammonoid life and habitat. In: Landman, N.H., Tanabe, K., Davis, R.A. (Eds.), Ammonoid Paleobiology, Topics in Geobiology 13, pp. 607–707.
Westermann, G.E.G., 2000. Marine faunal realms of the Mesozoic: review and revision under the new guidelines for biogeographic classification and nomenclature. Palaeogeography, Palaeoclimatology, Palaeoecology 163, 49–68.
Witam, O., 1998. Le Barrémien-Aptien de l'Atlas Occidental (Maroc) : lithostratigraphie, biostratigraphie, sédimentologie, stratigraphie séquentielle, géodynamique et paléontologie. Strata 30, 1–421.
Yamina, B., Ali Nabiha, B.H., Saloua, R., Kamal, T., 2002. Etude biostratigraphique du Crétacé inférieur (Barrémien supérieur- Albien) du Haut Atlas occidental (MAROC). Estudios Geologicos 58, 105–112.

Appendix A. Supplementary data

Supplementary data to this article can be found online at https://doi.org/10.1016/j.cretres.2018.09.007.